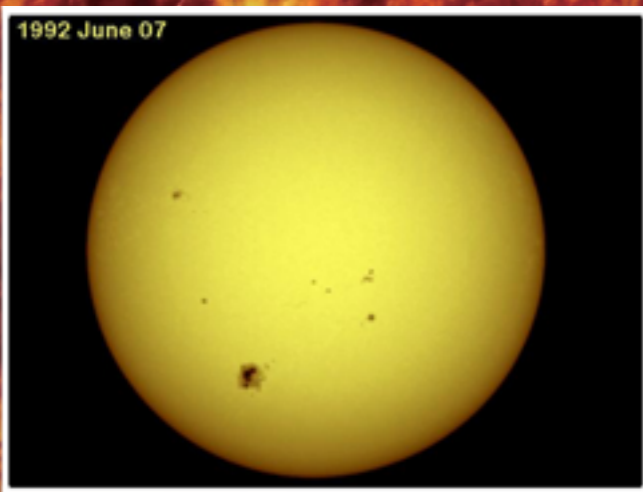
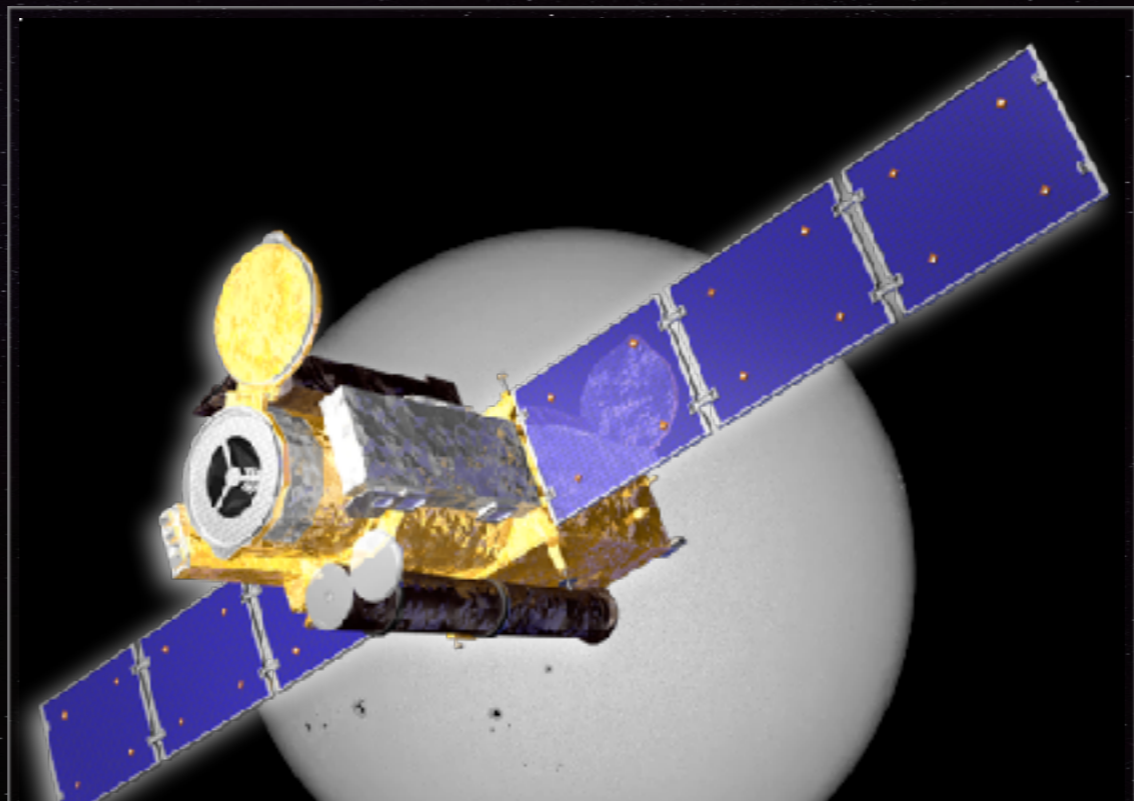
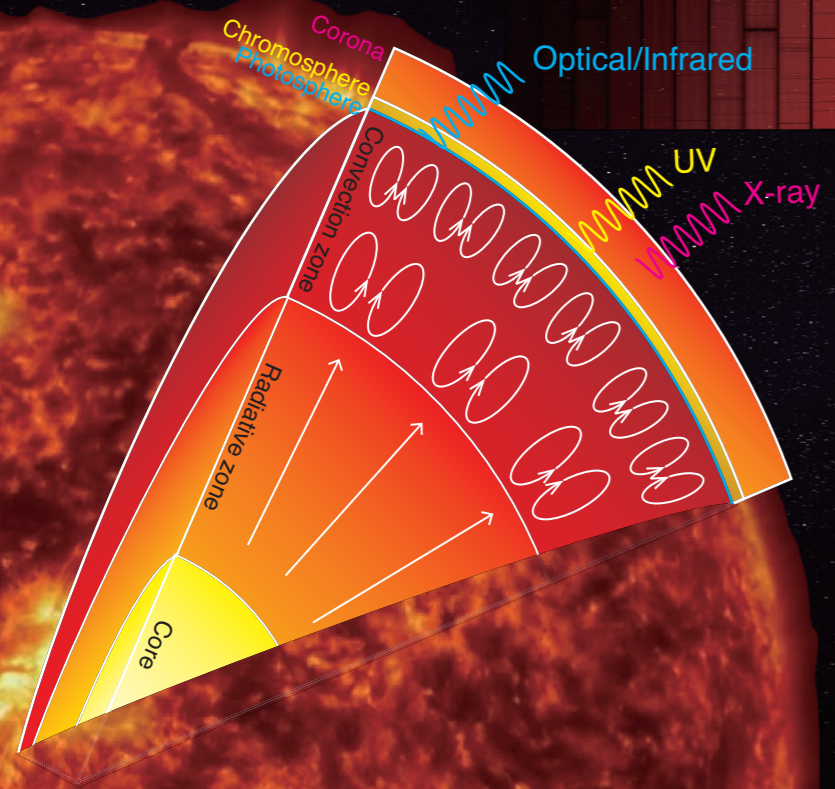


Vortices in the Solar Atmosphere (and Accretion Disks)

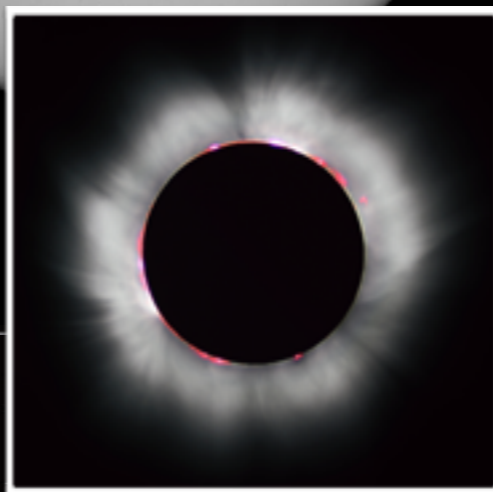
Yoshiaki Kato
(RIKEN)



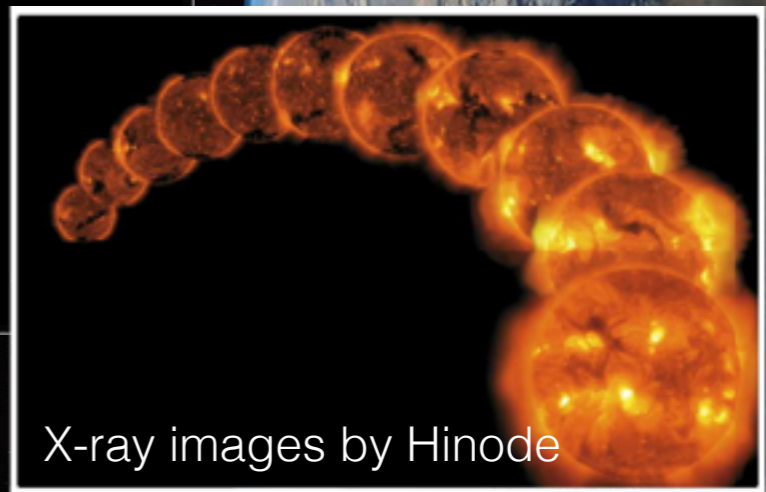
Photosphere
~ 5000 K



Chromosphere
~ 10000 K



Corona
~ 1 MK



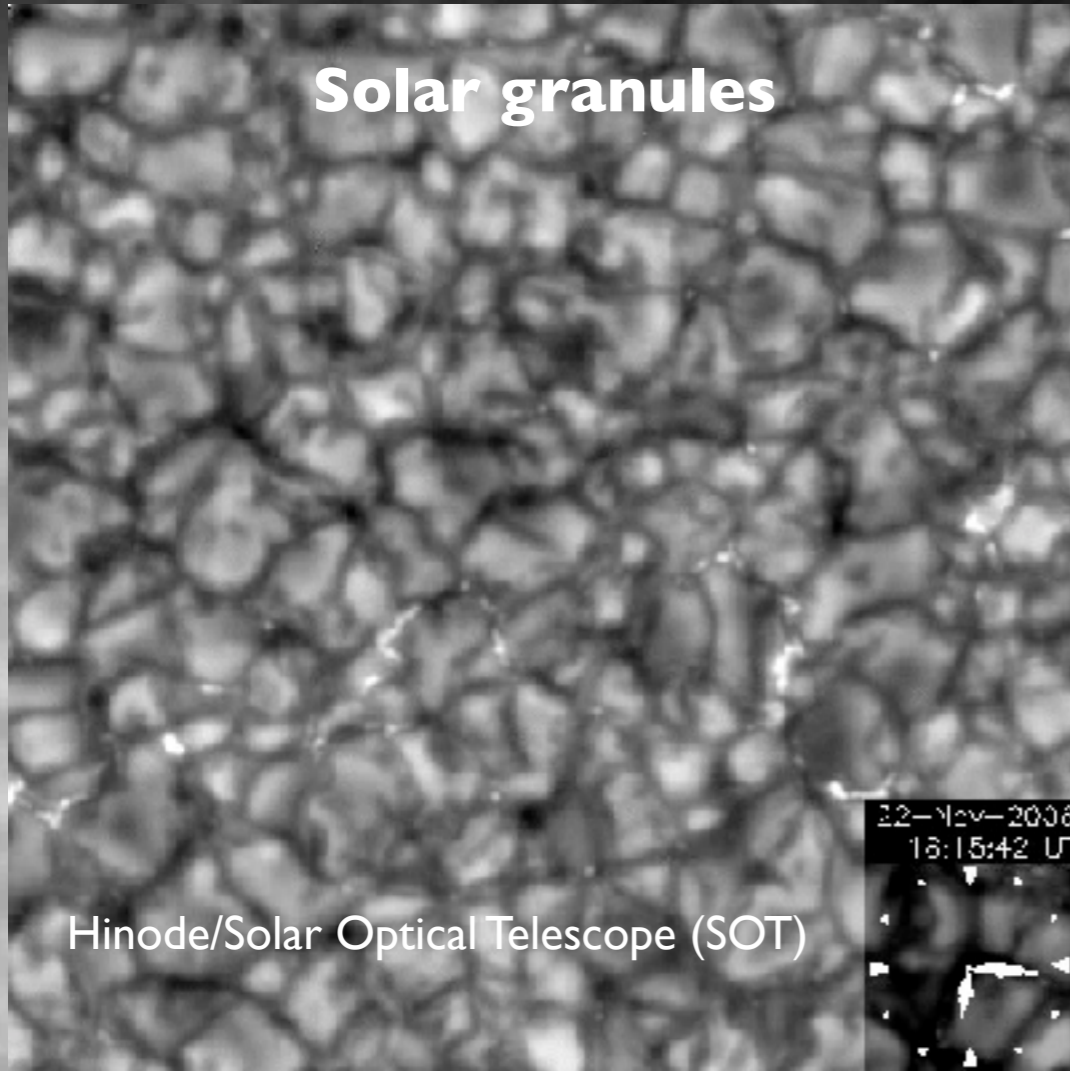
Solar Activity Cycle

Structure and Dynamics of the Solar Atmosphere

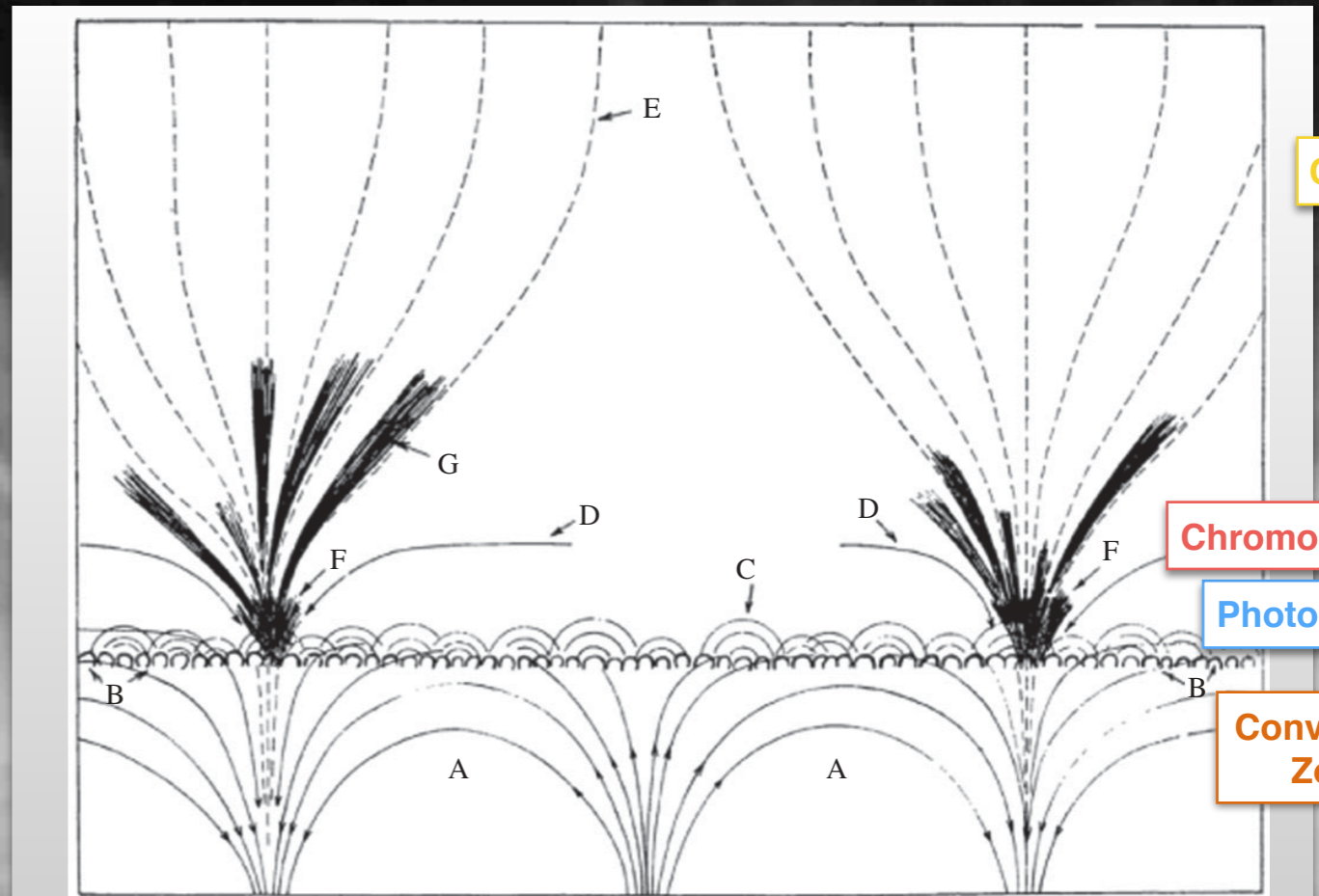
Solar Chromosphere

Spicules = Dynamical fibrils

Solar granules



Hinode/Solar Optical Telescope (SOT)



Corona

Chromosphere

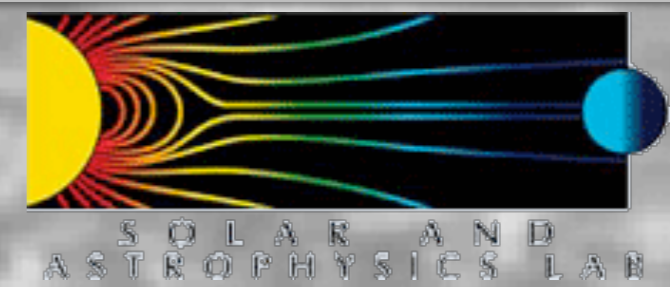
Photosphere

Convection Zone

Figure 1. Sketch of the granulation–supergranulation–spicule complex in cross section. A, Flow lines of a supergranulation cell. B, Photospheric granules. C, Wave motions. D, Large-scale chromospheric flow field seen in H α . E, [Magnetic] lines of force, pictured as uniform in the corona but concentrated at the boundaries of the supergranules in the photosphere and chromosphere. F, Base of a spicule ‘bush’ or ‘rosette’, visible as a region of enhanced emission in the H α and K-line cores. G, Spicules. [...] The distance between the bushes is 30 000 km. Reproduced with permission from Noyes [15], including this caption.

Rutten 2012

Hinode/Ca II H BFI movie
(courtesy by Mats Carlsson)



Radiation MHD equations

$$\frac{\partial \rho}{\partial t} = -\nabla \cdot (\rho v)$$

$$\frac{\partial \rho v}{\partial t} = -\nabla \cdot \left[\rho v v + \left(p + \frac{B^2}{2\mu} \right) \mathbf{I} - \frac{B B}{\mu} \right] + \rho g$$

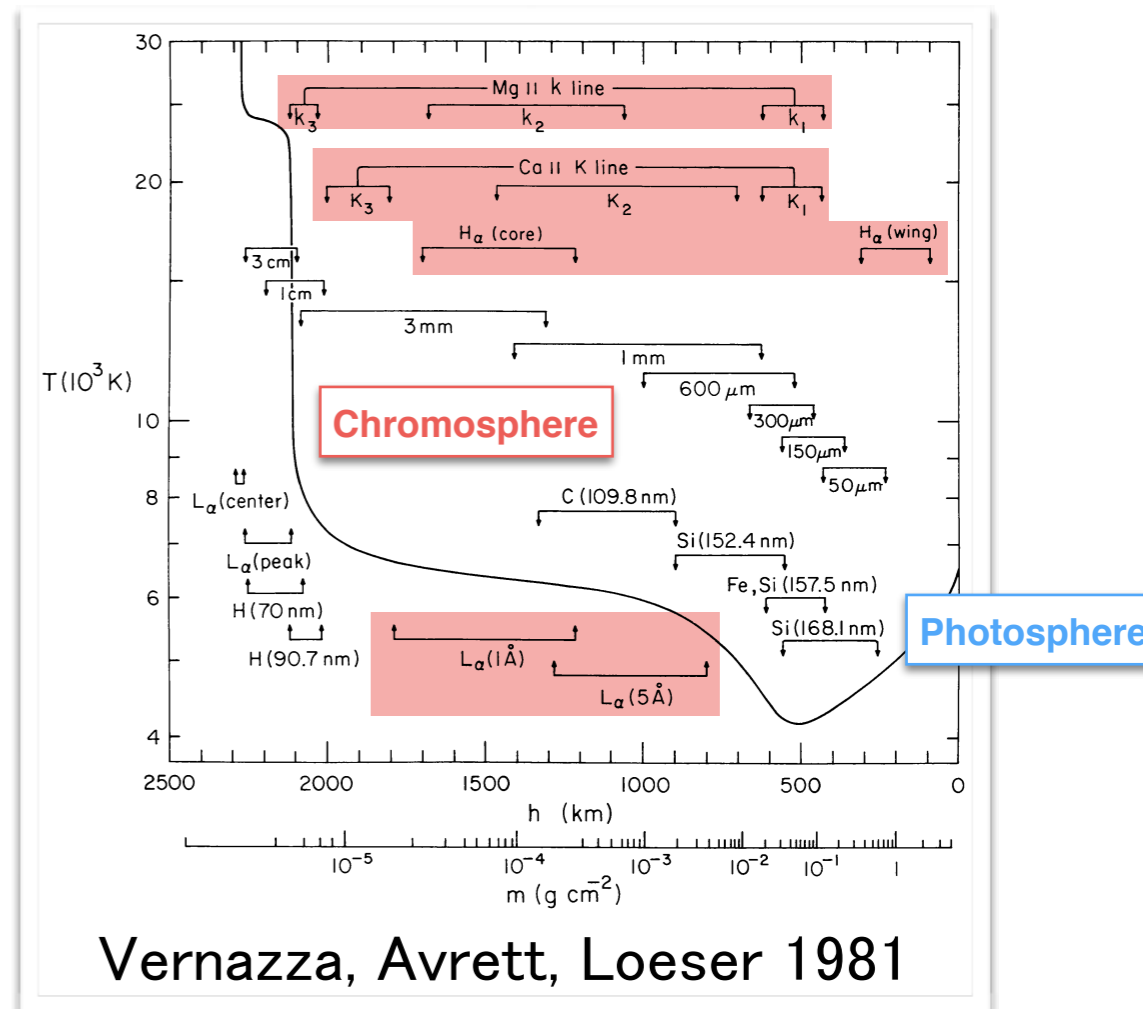
$$\frac{\partial \epsilon}{\partial t} = -\nabla \cdot \left[\left(\epsilon + p + \frac{B^2}{2\mu} \right) v - \frac{B (B \cdot v)}{\mu} \right] + \rho v \cdot g + Q$$

$$\frac{\partial B}{\partial t} = -\nabla \times E \quad E = -v \times B + \eta J \quad J = \frac{\nabla \times B}{\mu}$$

$$e = \rho \epsilon + \frac{1}{2} \rho v^2 + \frac{B^2}{2\mu}$$

$p = p(\rho, \epsilon)$ in LTE and Non-LTE

$$Q = Q_{\text{rad}} + Q_{\text{cond}}$$



Empirical radiative loss in the chromosphere: 2.5 - 4.3 kWm⁻² (Ulmschneider 1974; Vernazza et al. 1981)

Radiation transfer equation
Population density equation

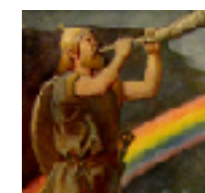
$$\frac{dI}{d\tau} = S - I$$

$$S_l = \frac{n_j A_{ji} \Psi}{n_i B_{ij} \Phi - n_j B_{ji} \Psi_{se}}$$

$$\frac{Dn_i}{Dt} = \sum_{j \neq i}^N n_j P_{ji} - n_i \sum_{j \neq i}^N P_{ij}$$

P_{ij} is the probability for a transition from level i to level j

Bifrost code
(Gudiksen et al. 2011)



- Finite-difference MHD solver
- Realistic EOS with Hydrogen ionisation
- Radiative transfer:
 - Optically thin radiative transfer (mostly in the corona),
 - Chromospheric radiation approximation (Leenaarts et al. 2007),
 - Full radiative transfer in the photosphere.
- Thermal conduction in the lower corona

Modeling a magnetic flux tube/sheath for investigating dynamical fibrils

Current sheets will form at the boundary of field lines.

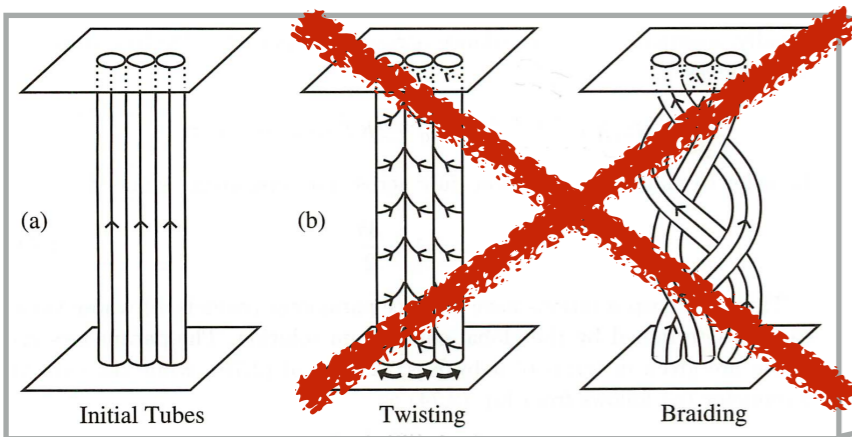
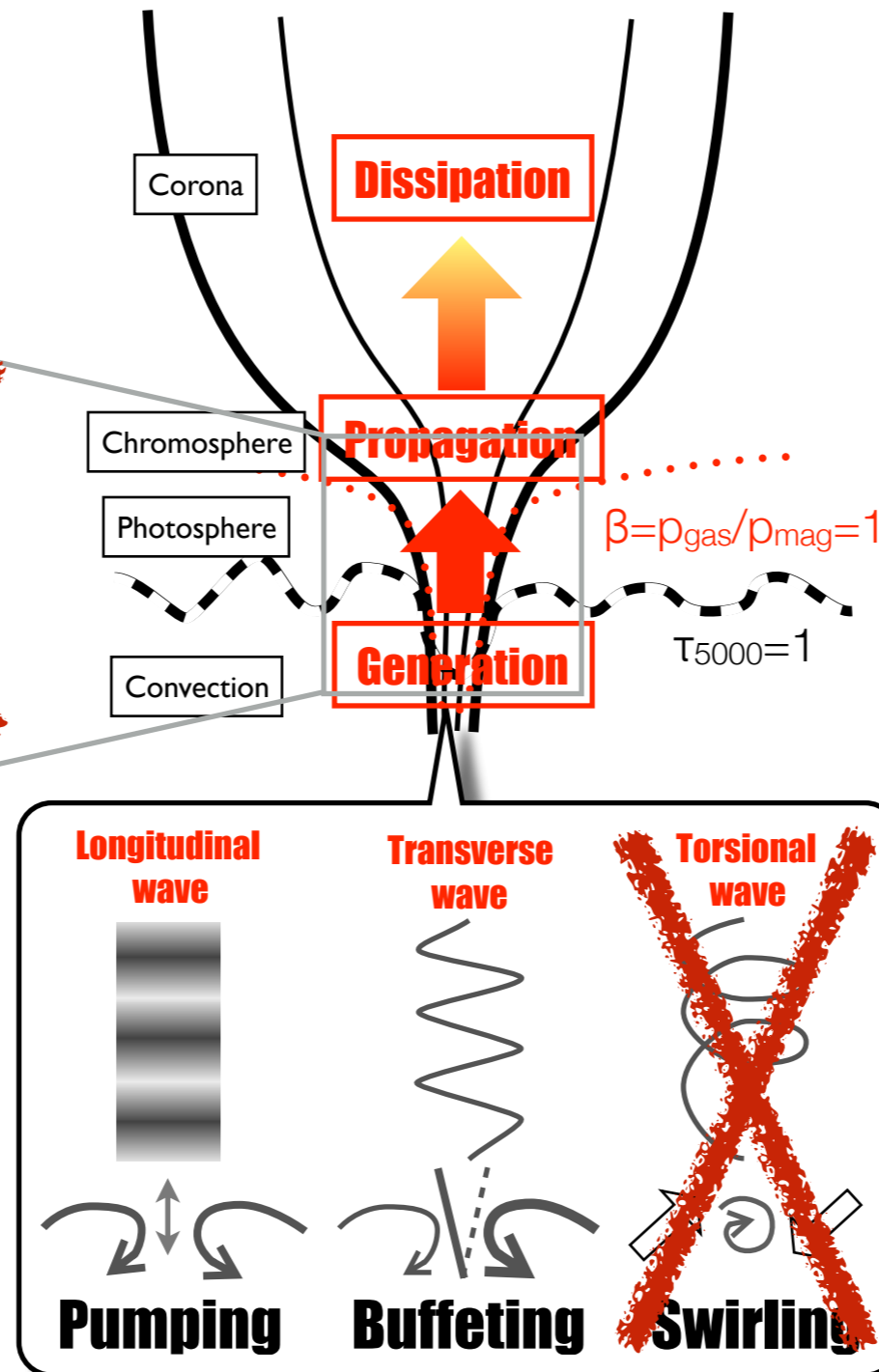


Fig. 2.16. The effect on (a) an initial field of (b) twisting and (c) braiding motions.

Parker 1979, 1990

Magnetic reconnections

Two-dimensional RMHD simulations



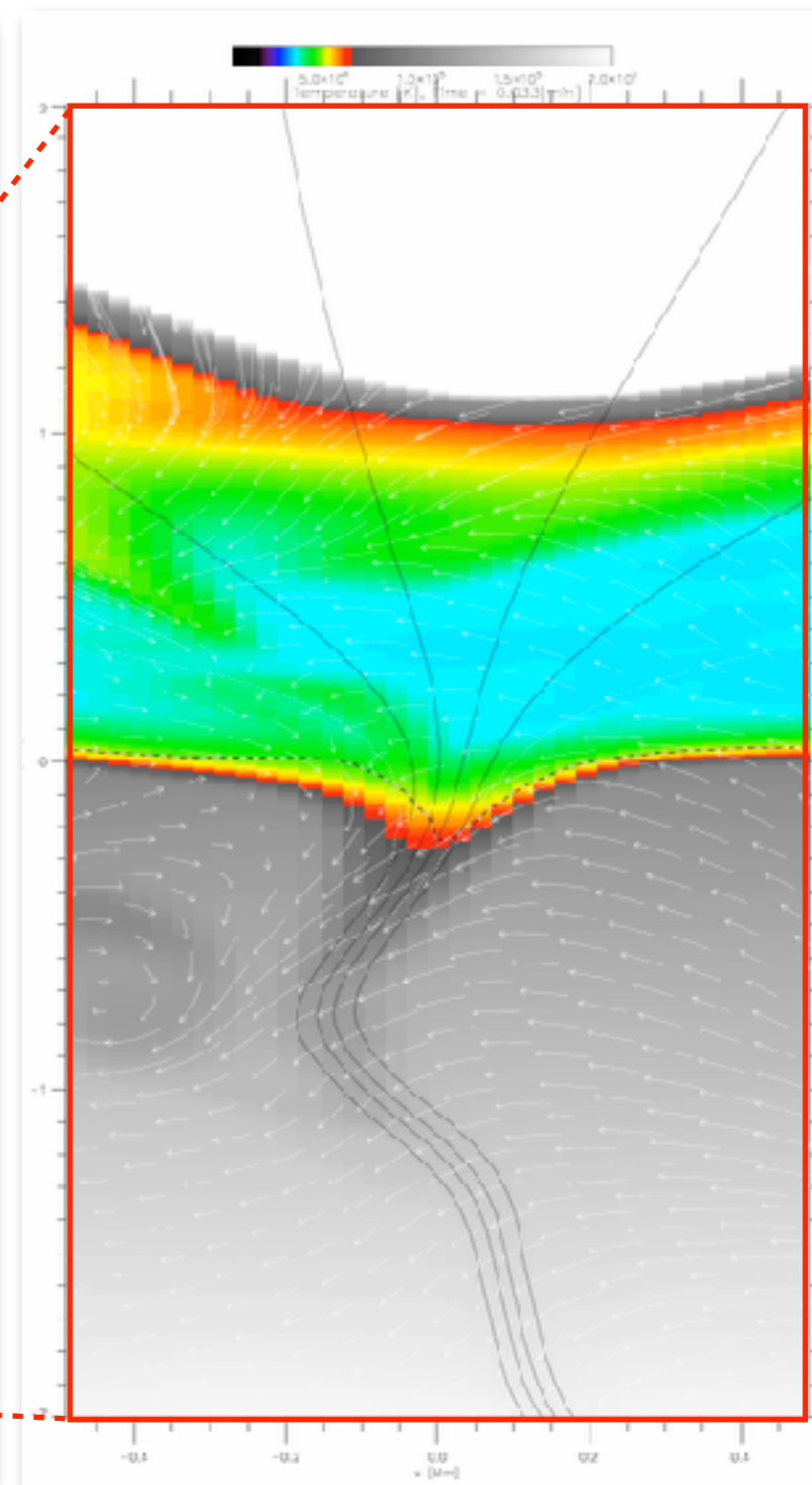
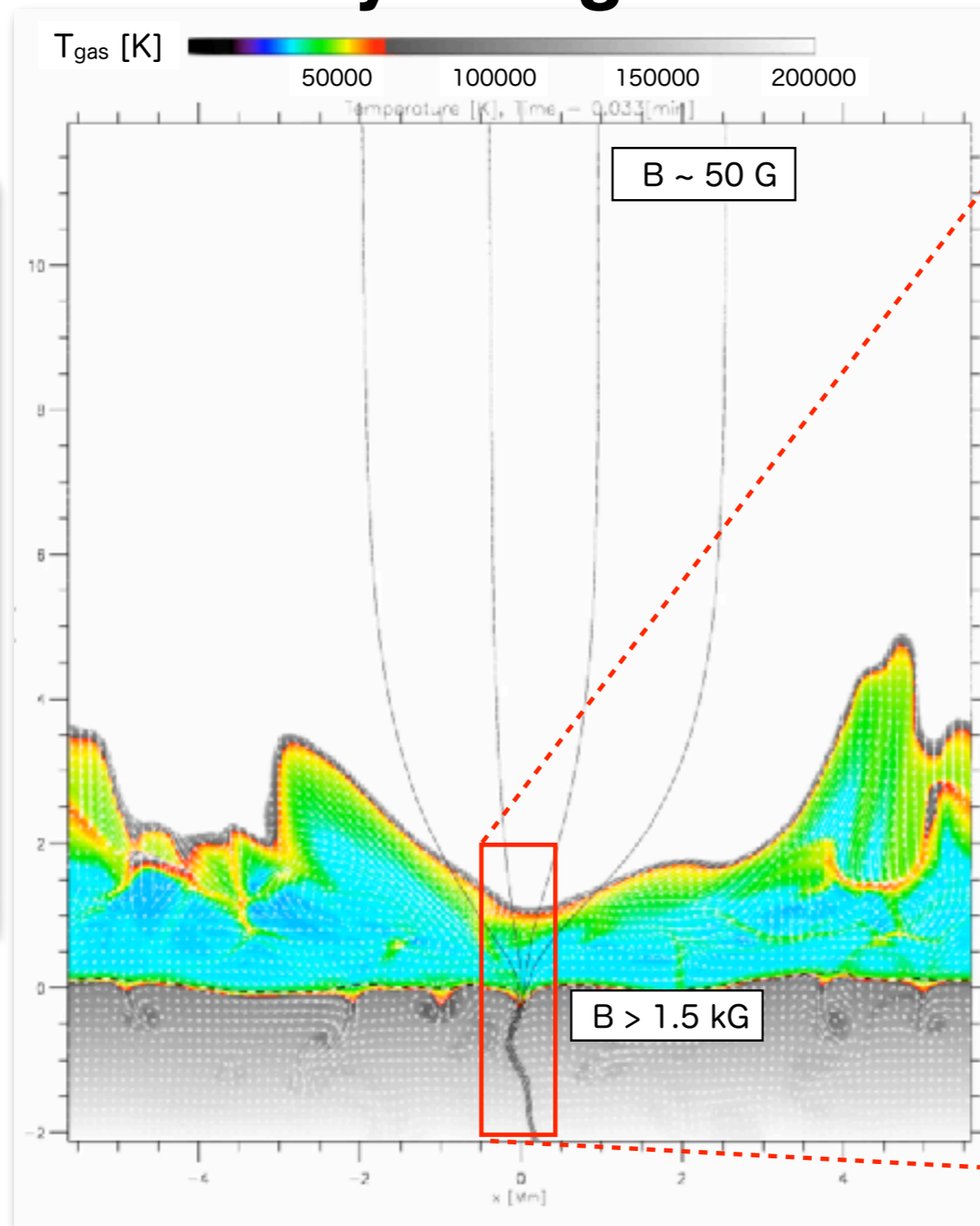
Rae & Roberts 1982

$$\frac{\partial^2 Q}{\partial t^2} - c_T^2 \frac{\partial^2 Q}{\partial z^2} + \omega_v^2 Q = 0 \quad \text{Klein-Gordon Equation}$$

Plane-parallel wave solution: $Q(z, t) \propto e^{i(\omega t - kz)}$
 where $\omega_v^2 = N_0 + \left(\frac{3}{4} - \frac{1}{\gamma}\right)^2 \frac{c_T^2}{H^2}$, $Q(z, t) = e^{-z/4H} v(z, t)$
 the Brunt-Väisälä frequency: $N_0^2(z) = -g \left(\frac{1}{\rho_0} \frac{d\rho_0}{dz} + \frac{g}{c_0^2} \right)$
 the tube speed: $c_T = \frac{c_s c_A}{\sqrt{c_s^2 + c_A^2}}$
 $\omega^2 = k^2 c_T^2 + \omega_v^2$
 $k^2 = \frac{\omega^2 - \omega_v^2}{c_T^2}$, $\omega = \pm \omega(k) = \pm (\omega_v^2 + k^2 c_T^2)^{1/2}$
 $\omega < \omega_v$: evanescent $\omega > \omega_v$: wave propagation

- Two possible solutions:**
1. Forced oscillations above the cutoff frequency
 → Continuous driving
 2. Resonant oscillations near the cutoff frequency
 → Impulsive driving

“Realistic” modeling of the solar atmosphere by using Bifrost

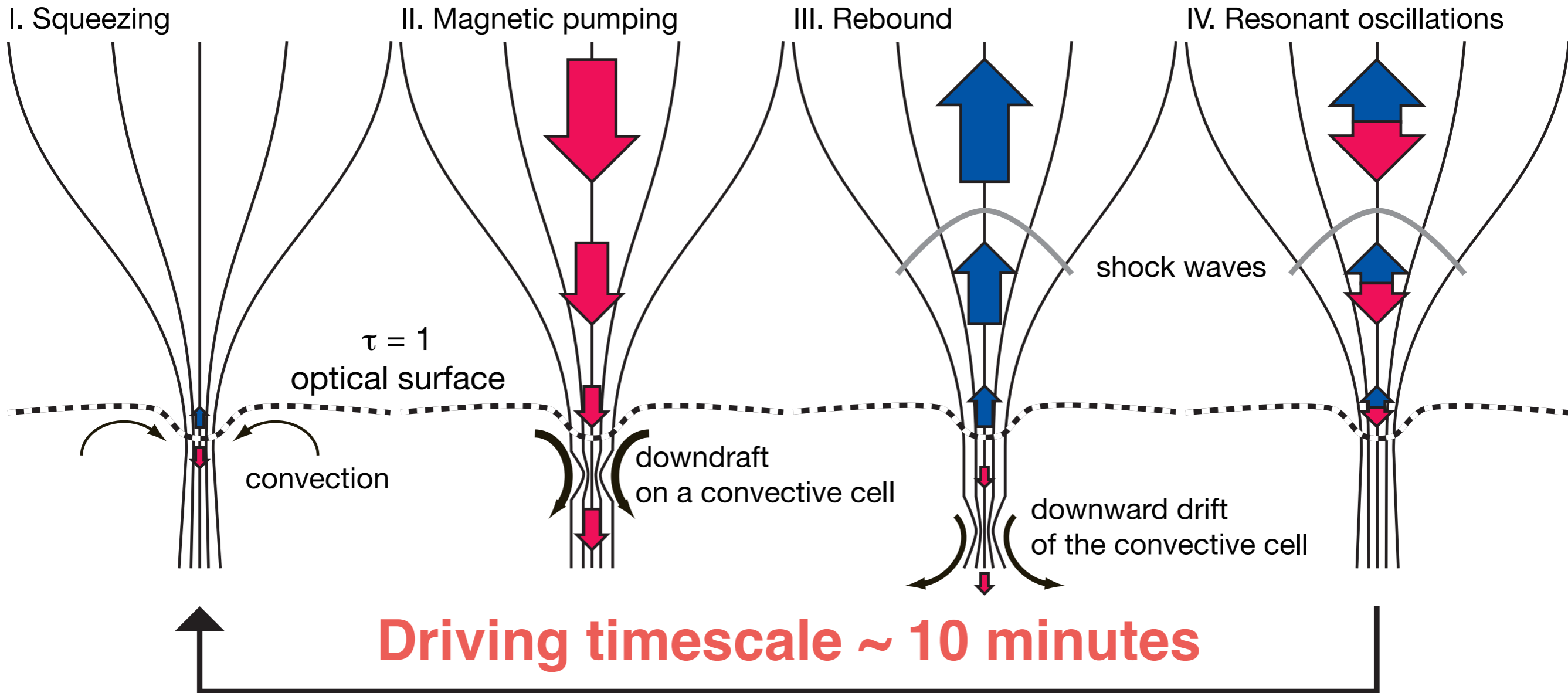


- Bifrost code**
(Gudiksen et al. 2011)
- Finite-difference MHD solver
 - Realistic EOS with Hydrogen ionisation
 - Radiative transfer:
 - Optically thin radiative transfer (mostly in the corona),
 - Chromospheric radiation approximation (Leenaarts et al. 2007),
 - Full radiative transfer in the photosphere.
 - Thermal conduction in the lower corona

$\Delta X=28\text{km}$
 $N_x=400 N_z=535$

Magnetic pumping mechanism for sustaining the solar chromosphere

Chromospheric response
~ 4 minutes



Summary

Magnetic pumping is responsible for “dynamic fibrils”

Current sheets will form at the boundary of field lines.

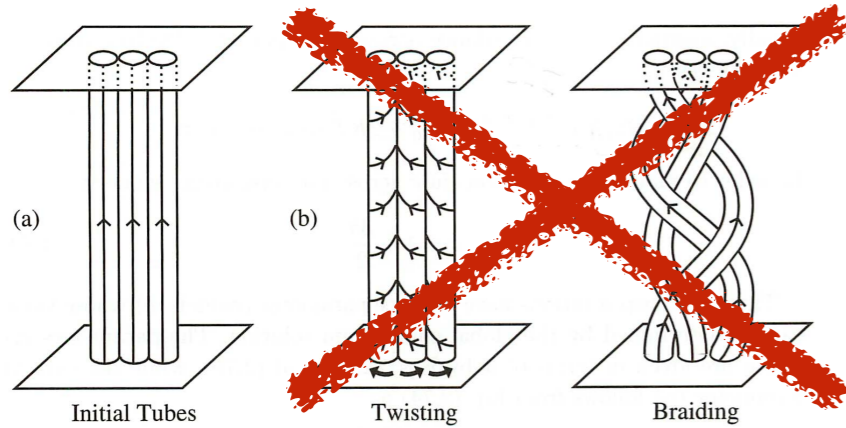
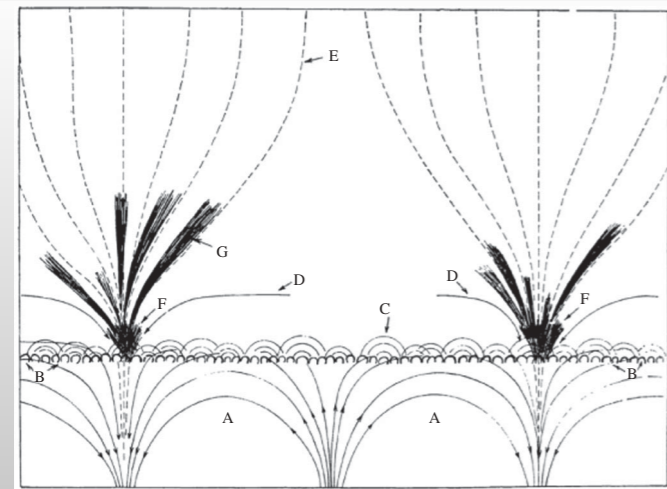
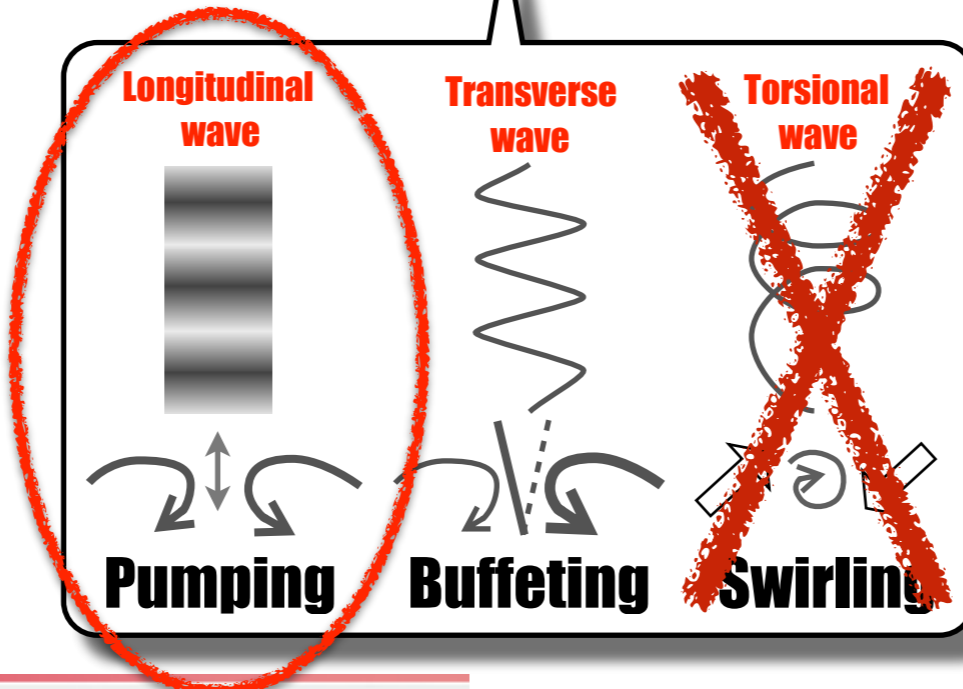
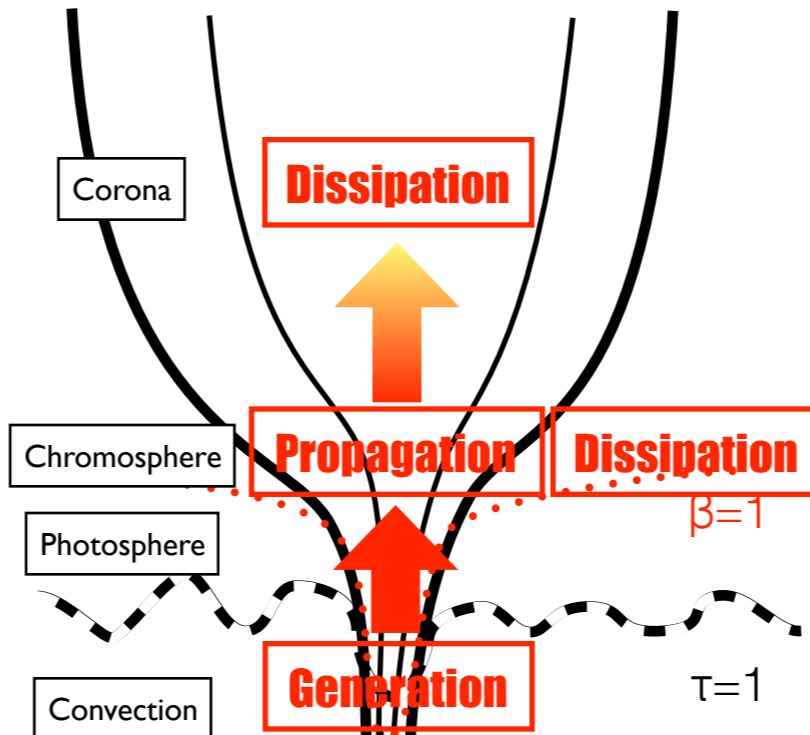


Fig. 2.16. The effect on (a) an initial field of (b) twisting and (c) braiding motions.



Rutten 2012

Recurrent shock waves can sustain solar chromosphere



Rae & Roberts 1982

$$\frac{\partial^2 Q}{\partial t^2} - c_T^2 \frac{\partial^2 Q}{\partial z^2} + \omega_v^2 Q = 0 \quad \text{Klein-Gordon Equation}$$

Plane-parallel wave solution: $Q(z, t) \propto e^{i(\omega t - kz)}$
 where $\omega_v^2 = N_0 + \left(\frac{3}{4} - \frac{1}{\gamma}\right)^2 \frac{c_T^2}{H^2}$, $Q(z, t) = e^{-z/4H} v(z, t)$
 the Brunt-Väisälä frequency: $N_0^2(z) = -g \left(\frac{1}{\rho_0} \frac{d\rho_0}{dz} + \frac{g}{c_0^2} \right)$
 the tube speed: $c_T = \frac{c_s c_A}{\sqrt{c_s^2 + c_A^2}}$
 $\omega^2 = k^2 c_T^2 + \omega_v^2$
 $k^2 = \frac{\omega^2 - \omega_v^2}{c_T^2}$, $\omega = \pm \omega(k) = \pm (\omega_v^2 + k^2 c_T^2)^{1/2}$
 $\omega < \omega_v$: evanescent $\omega > \omega_v$: wave propagation

Two possible solutions:

1. Forced oscillations above the cutoff frequency
 → Continuous driving
2. Resonant oscillations near the cutoff frequency
 → Impulsive driving

References

- Kato, Y., Steiner, O., Steffen, M., Suematsu, Y., *Excitation of slow-modes in network magnetic elements through magnetic pumping*, 2011, ApJ, **730**, L24-L28
- Kato, Y., Steiner, O., Hansteen, V., Gudiksen, B., Wedemeyer, B., Carlsson, M., *Chromospheric and Coronal Wave Generation in a Magnetic Flux Sheath*, 2016, ApJ, **827**, 7-23
- Quintero Noda, C., Kato, Y., Katsukawa, Y., Oba, T., de la Cruz Rodríguez, J., Carlsson, M., Shimizu, T., Orozco Suárez, D., Ruiz Cobo, B., Kubo, M., Anan, T., Ichimoto, K., Suematsu, Y.; *Chromospheric polarimetry through multiline observations of the 850-nm spectral region – II. A magnetic flux tube scenario*, 2017, MNRAS, **472**, 727–737

Hunting for Solar Tornadoes

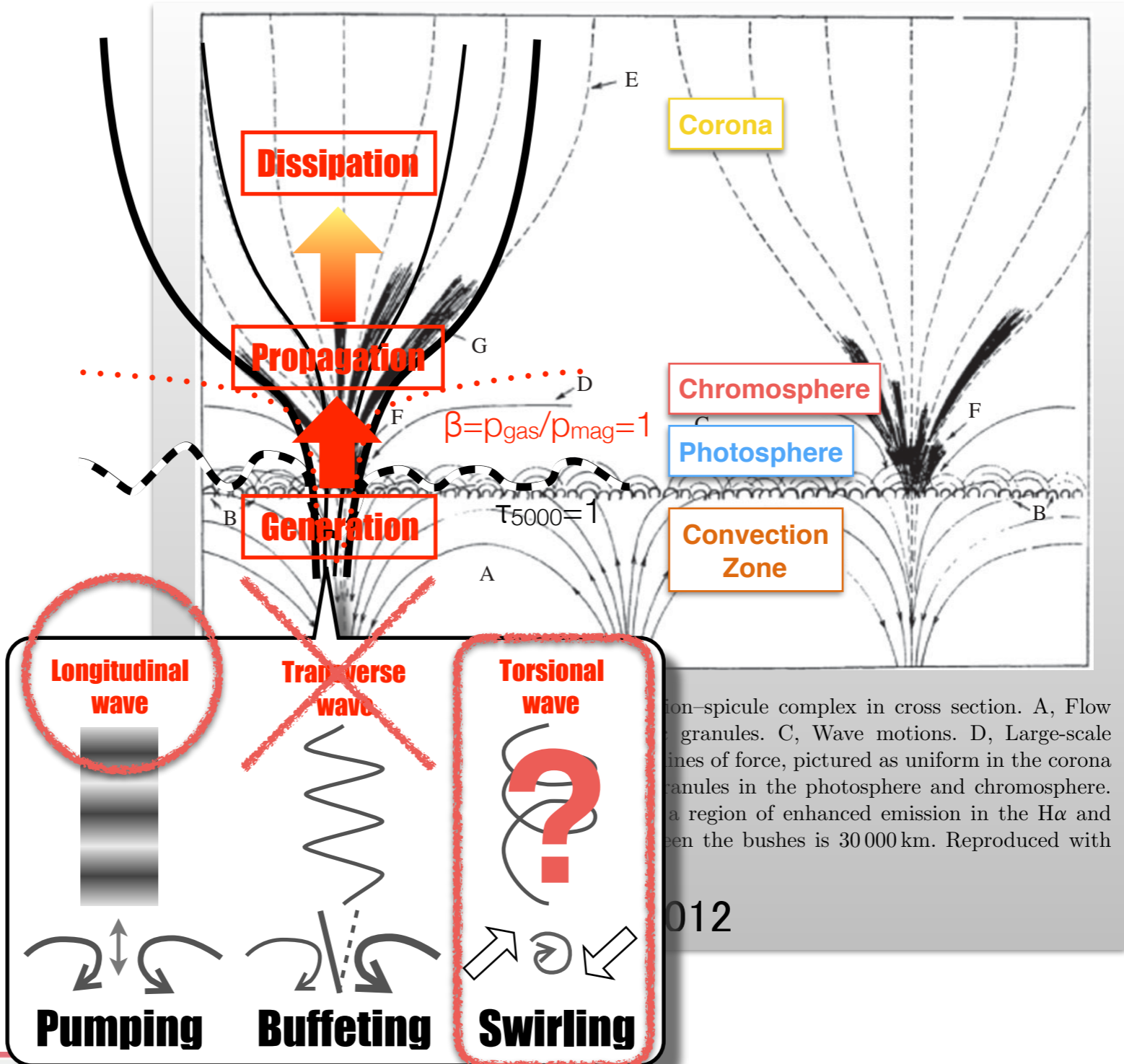
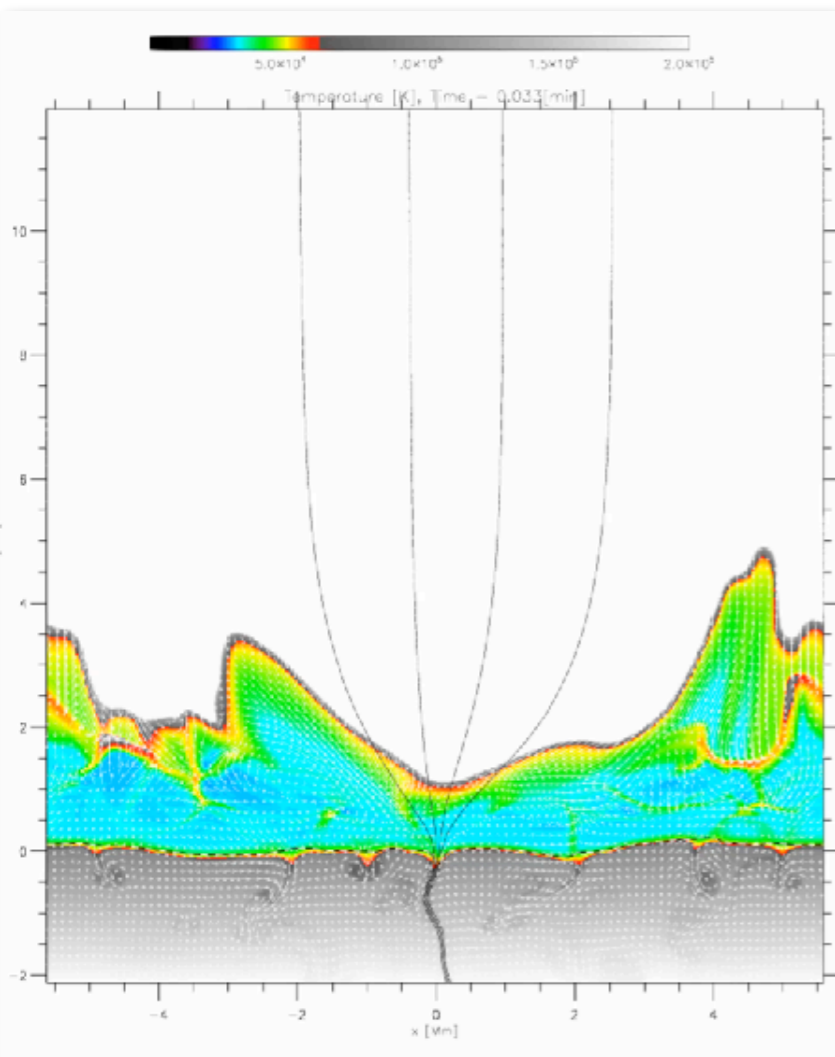
Vincent van Gogh's *The Starry Night* (1889)
the view from the window of his asylum room at Saint-Rémy-de-Provence

Yoshiaki Kato
(University of Oslo → RIKEN)

Sven Wedemeyer
(University of Oslo)

Magnetic flux tube

a magnetic portal for energy transport

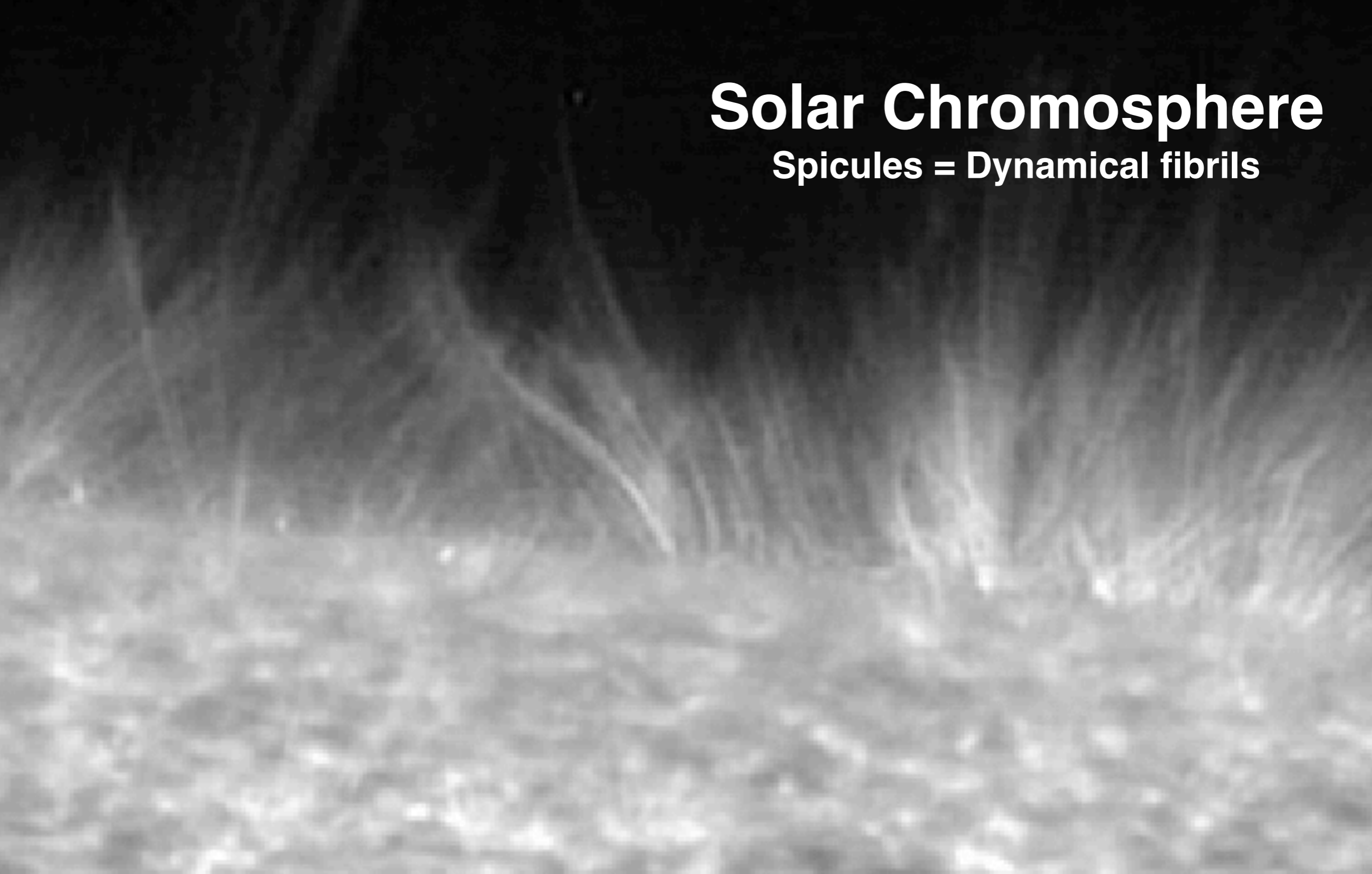


YK et al. 2016

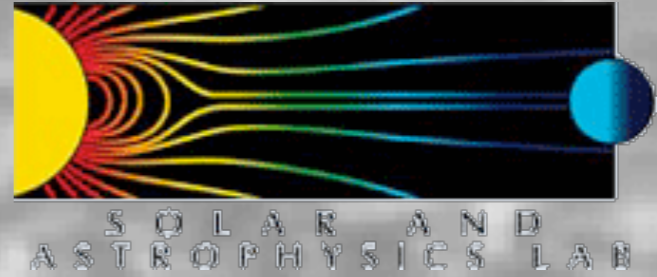
on-spicule complex in cross section. A, Flow granules. C, Wave motions. D, Large-scale lines of force, pictured as uniform in the corona granules in the photosphere and chromosphere. a region of enhanced emission in the H α and between the bushes is 30 000 km. Reproduced with 012

Solar Chromosphere

Spicules = Dynamical fibrils

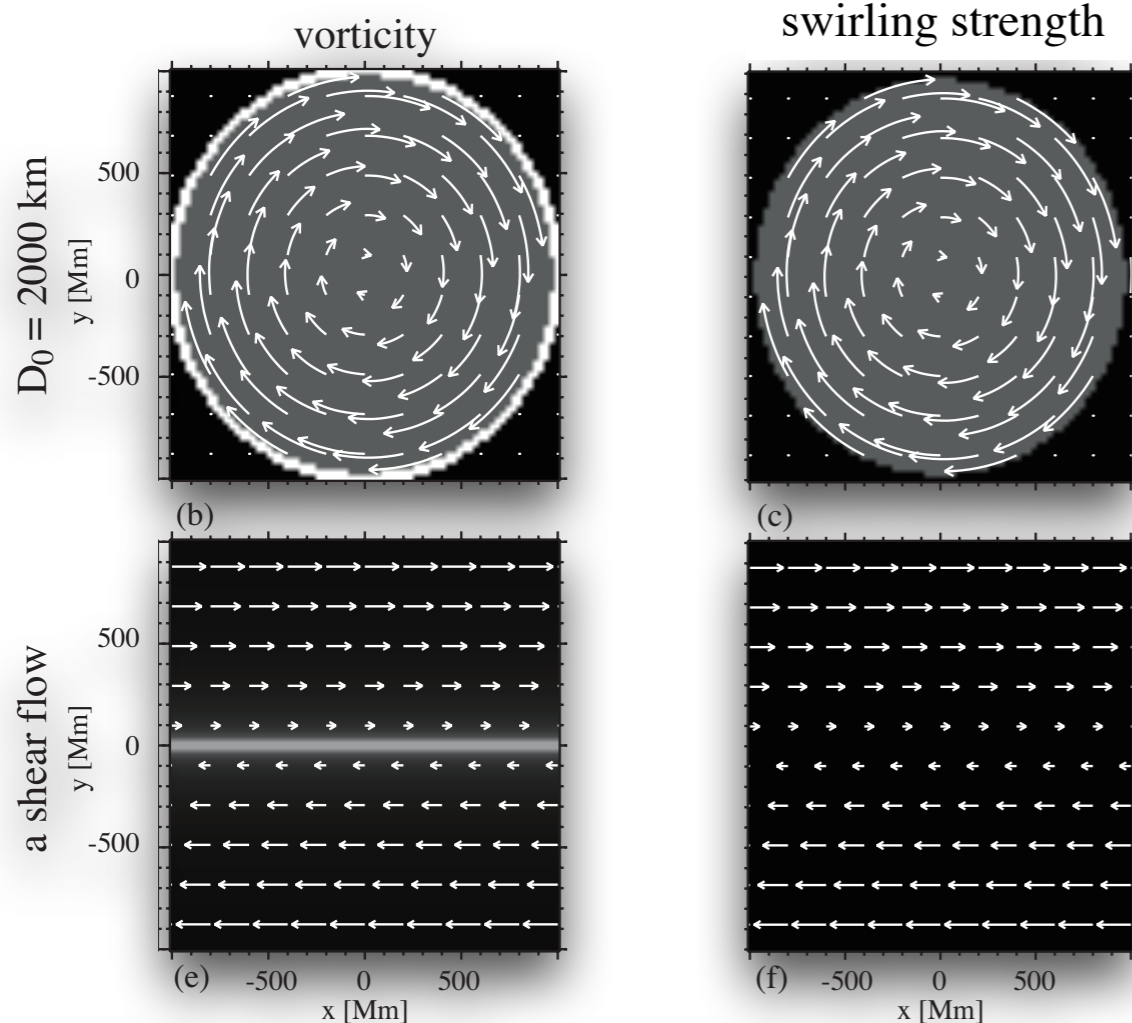
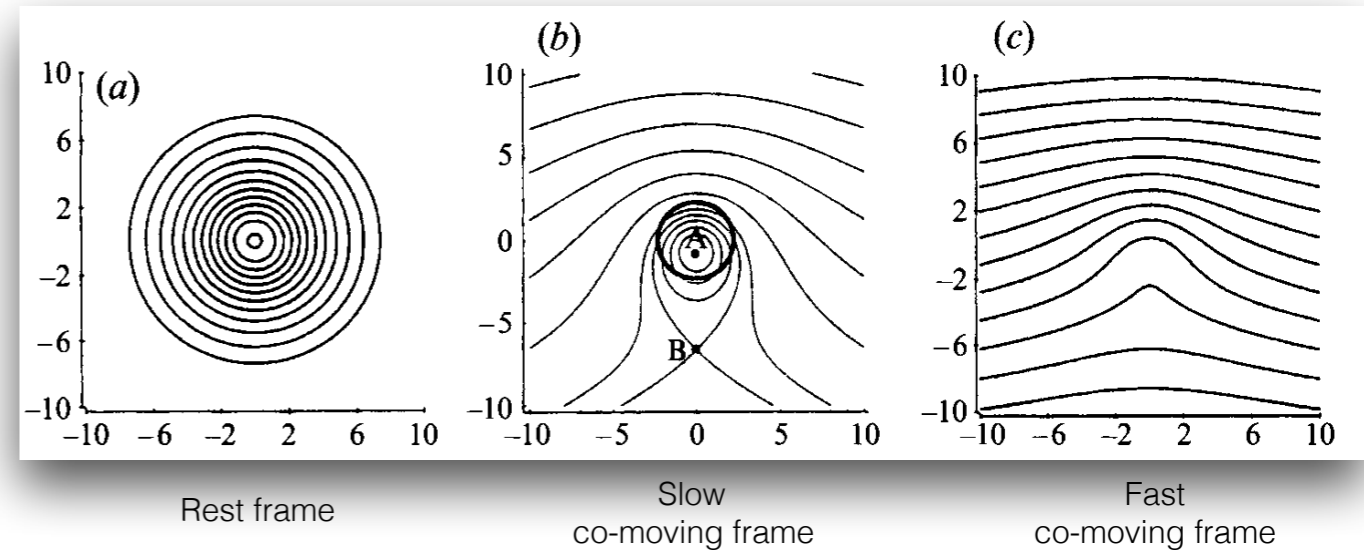


Hinode/Ca II H BFI movie
(courtesy by Mats Carlsson)



How to find a vortical structure?

- Streamlines
- Vorticity magnitude $\nabla \times \mathbf{v} = \omega$
- Local pressure minimum



①

$-\nabla P$ $\frac{v^2}{r}$ (centrifugal force)

if low Re, $-\nabla P \sim \nu \nabla^2 v$ (viscous force)

$(Re = \frac{\rho v L}{\nu})$

② $\nabla^2 p = -\rho \kappa_{ij} u_{ji}$ (no gravity)

"Poisson Eqn"

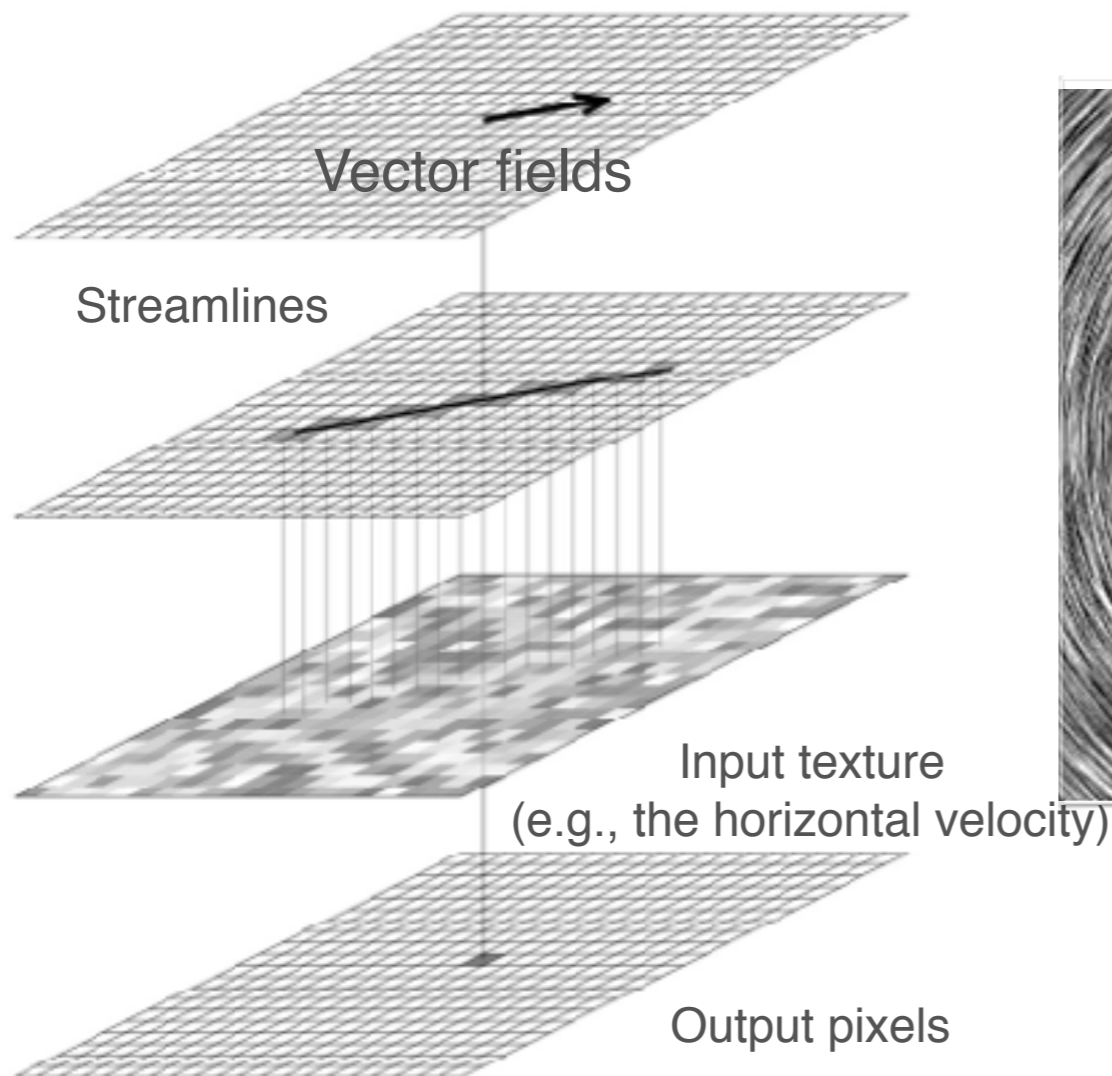
$\nabla \cdot \mathbf{g} = -4\pi G \rho$ $\nabla^2 \phi = 4\pi G \rho \rightarrow \frac{\partial \phi}{\partial r} = -\frac{GM}{r}$

$\mathbf{g} = -\nabla \phi$

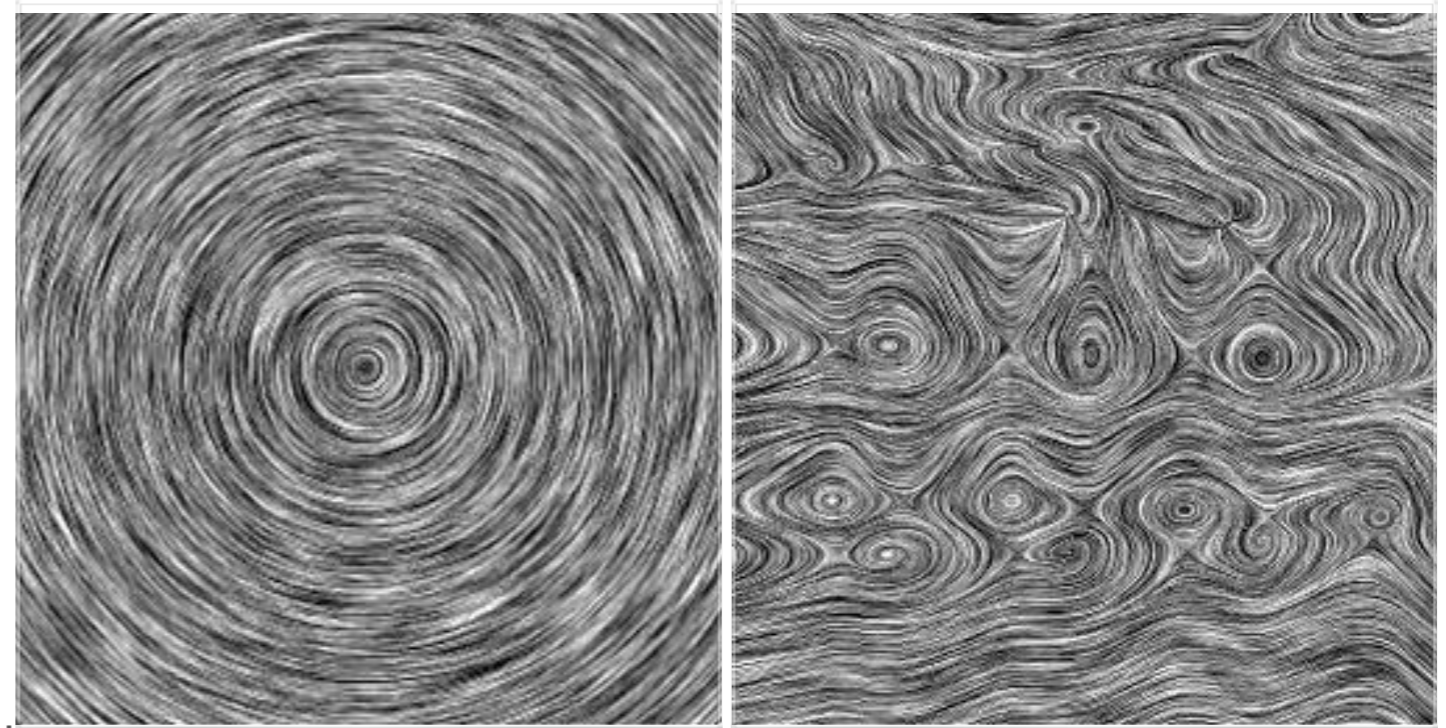
no characteristic radius.

Fancy illustration of vortical structure

Line Integral Convolution (LIC)



Examples



Visualization of vortical flows
by using LIC imaging

Cabral & Leedom SIGGRAPH'93

What's a definition of a vortex?

J. Fluid Mech. (1995), vol. 285, pp. 69–94
 Copyright © 1995 Cambridge University Press

69

On the identification of a vortex

By JINHEE JEONG AND FAZLE HUSSAIN

Department of Mechanical Engineering, University of Houston, Houston, TX 77204-4792, USA

(Received 6 December 1993 and in revised form 4 July 1994)

Considerable confusion surrounds the longstanding question of what constitutes a vortex, especially in a turbulent flow. This question, frequently misunderstood as academic, has recently acquired particular significance since coherent structures (CS) in turbulent flows are now commonly regarded as vortices. An objective definition of a vortex should permit the use of vortex dynamics concepts to educe CS, to explain formation and evolutionary dynamics of CS, to explore the role of CS in turbulence phenomena, and to develop viable turbulence models and control strategies for turbulence phenomena. We propose a definition of a vortex in an incompressible flow in terms of the eigenvalues of the symmetric tensor $\mathbf{S}^2 + \mathbf{\Omega}^2$; here \mathbf{S} and $\mathbf{\Omega}$ are respectively the symmetric and antisymmetric parts of the velocity gradient tensor $\nabla \mathbf{u}$. This definition captures the pressure minimum in a plane perpendicular to the vortex axis at high Reynolds numbers, and also accurately defines vortex cores at low Reynolds numbers, unlike a pressure-minimum criterion. We compare our definition with prior schemes/definitions using exact and numerical solutions of the Euler and Navier–Stokes equations for a variety of laminar and turbulent flows. In contrast to definitions based on the positive second invariant of $\nabla \mathbf{u}$ or the complex eigenvalues of $\nabla \mathbf{u}$, our definition accurately identifies the vortex core in flows where the vortex geometry is intuitively clear.

1. Introduction

The concept of vortices is as old as the subject of hydrodynamics; yet, an accepted definition of a *vortex* is still lacking. Turbulence is viewed as a tangle of vortex filaments, and much of turbulence physics is well explained using the concepts of vortex dynamics (e.g. see Tennekes & Lumley 1972; Hunt 1987). Turbulent shear flows have been found to be dominated by spatially coherent, temporarily evolving vortical motions, popularly called *coherent structures* (CS) (Cantwell 1981; Lumley 1981; Hussain 1980). Vortex dynamics, which govern the evolution and interaction of CS and coupling of CS with background turbulence, is promising not only for understanding

1. Introduction

The concept of vortices is as old as the subject of hydrodynamics; yet, an accepted definition of a *vortex* is still lacking. Turbulence is viewed as a tangle of vortex filaments, and much of turbulence physics is well explained using the concepts of vortex dynamics (e.g. see Tennekes & Lumley 1972; Hunt 1987). Turbulent shear flows have

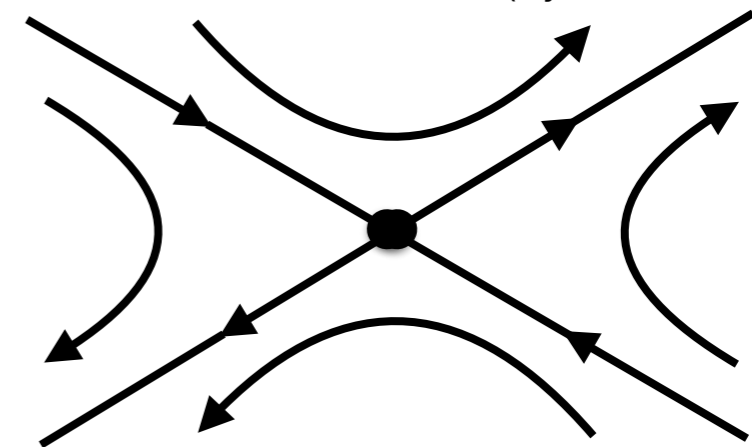
detectable regularity in time and space. Hence, a reference signal such as velocity can be used as a trigger for eduction (Hussain & Zaman 1980; Cantwell & Coles 1983).

Downloaded from <http://www.cambridge.org/core>. Universitetsbiblioteket i Oslo, on 20 Sep 2016 at 08:35:56, subject to the Cambridge Core terms of use, available at <http://www.cambridge.org/core/terms>. <http://dx.doi.org/10.1017/S0022112095000462>

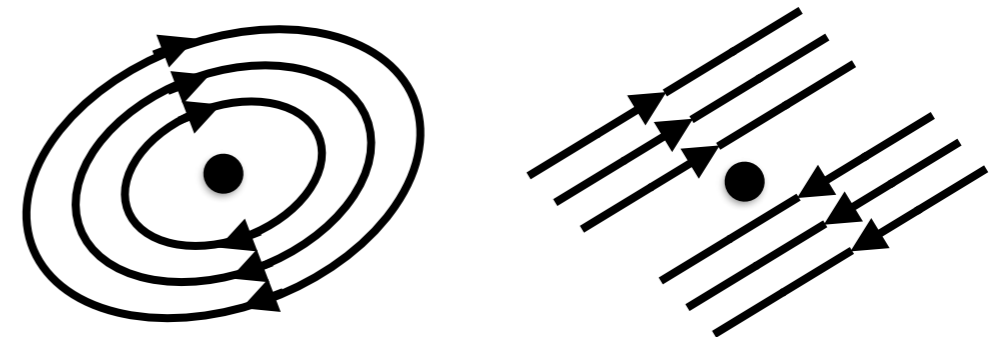
$$\nabla v = S + \Omega \quad \text{the velocity gradient tensor}$$

Galilean-invariants

$$S = \frac{1}{2} [\nabla v + (\nabla v)^T] \quad \text{the rate-of-strain tensor (symmetric part)}$$



$$\Omega = \frac{1}{2} [\nabla v - (\nabla v)^T] \quad \text{the vorticity tensor (Anti-symmetric part)}$$



Recent measures of a vortex

An imaginary part of eigenvalue of the velocity gradient tensor
 “Swirling Strength” (Moll et al. 2011)

Consider the velocity gradient tensor, \mathcal{D}_{ij}

$$\mathcal{D}_{ij} = \frac{\partial v_i}{\partial x_j} \quad (2)$$

If λ are the eigenvalues of \mathcal{D}_{ij} , then

$$[\mathcal{D}_{ij} - \lambda I] e = 0 \quad (3)$$

where e is the eigenvector.

The eigenvalues can be determined by solving the characteristic equation

$$\det[\mathcal{D}_{ij} - \lambda I] = 0 \quad (4)$$

which, for a velocity flow in two-dimensional space $\mathbf{v} = (v_x, v_y)$, can be written as

$$\lambda^2 + P\lambda + Q = 0 \quad (5)$$

where $P = -\text{tr}(\mathcal{D}_{ij})$ and $Q = \det(\mathcal{D}_{ij})$. Equation (5) has the following canonical solutions:

$$\lambda = \frac{-P \pm \sqrt{P^2 - 4Q}}{2} \quad (6)$$

The critical point analysis/classification on the differential equations

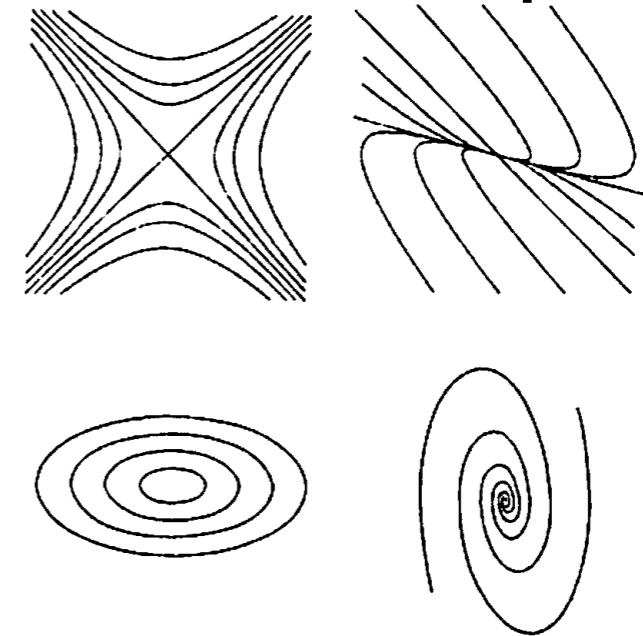


Figure 2.3

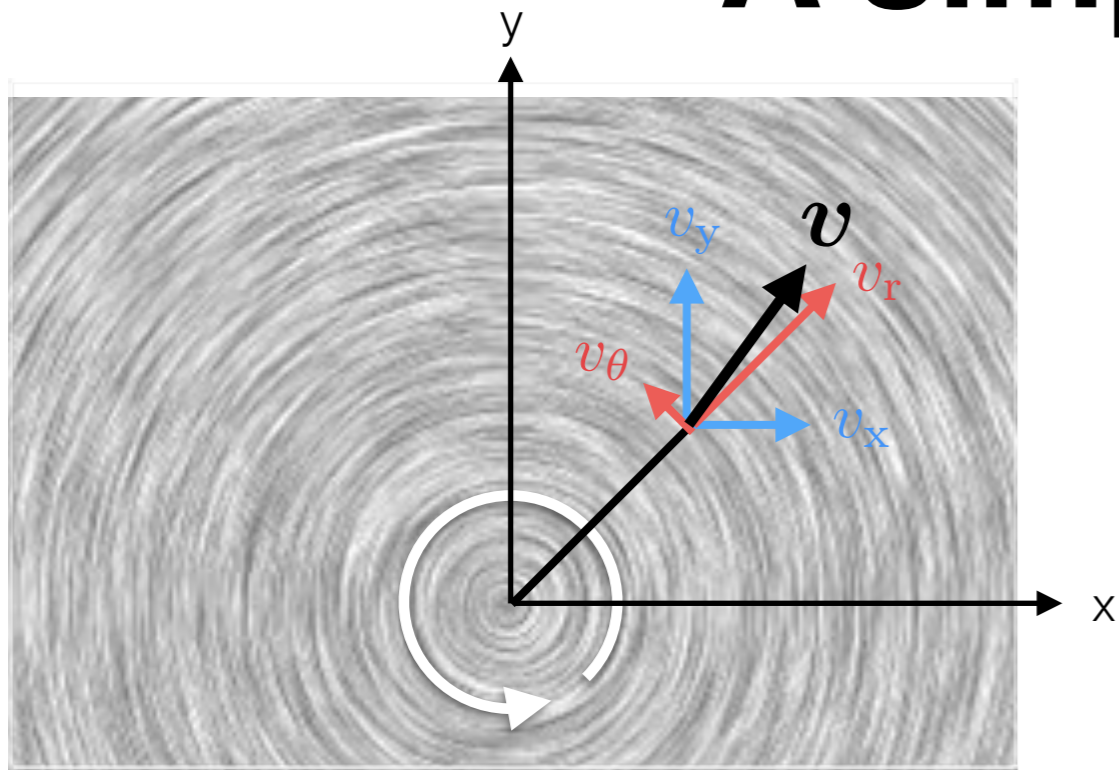
Types (topologies) of critical points. From top-left to bottom-right, types are saddle, node, center, and spiral.

Table 2.1 Roots and Types of Critical Points.

Roots	Type
Two real roots with opposite sign	saddle
Two real roots with same sign	node
Pure imaginary roots	center
Complex roots	spiral

“Black Hole Accretion Disks” 2008 p.66

A simple example



$$\lambda^2 + P\lambda + Q = 0$$

$$P = -\text{tr}(\mathcal{D}_{ij}) = \frac{(x+y)}{r^2} \mu$$

$$Q = \det(\mathcal{D}_{ij}) = \left(\frac{xy}{r^4}\right) \mu^2 + \nu^2$$

$$\lambda = \frac{-P \pm \sqrt{P^2 - 4Q}}{2}$$

- a pure circular flow

$$\mu = 0, \nu \neq 0 \longrightarrow P = 0, Q = \nu^2$$

a conjugate pair of complex roots of $\lambda = \pm i\nu$

$$\begin{bmatrix} v_x \\ v_y \end{bmatrix} = \begin{bmatrix} \cos \theta & -\sin \theta \\ \sin \theta & \cos \theta \end{bmatrix} \begin{bmatrix} v_r \\ v_\theta \end{bmatrix}$$

$$(v_r, v_\theta) = (\mu, r\nu) \text{ where } r = \sqrt{x^2 + y^2}$$

$$\mathbf{v} = \left[\mu \left(\frac{x}{r} \right) - \nu y \right] \mathbf{e}_x + \left[\mu \left(\frac{y}{r} \right) + \nu x \right] \mathbf{e}_y$$

$$\longrightarrow \mathcal{D}_{ij} = \begin{bmatrix} \mu \left(\frac{x}{r^2} \right) & -\nu \\ \nu & \mu \left(\frac{y}{r^2} \right) \end{bmatrix}$$

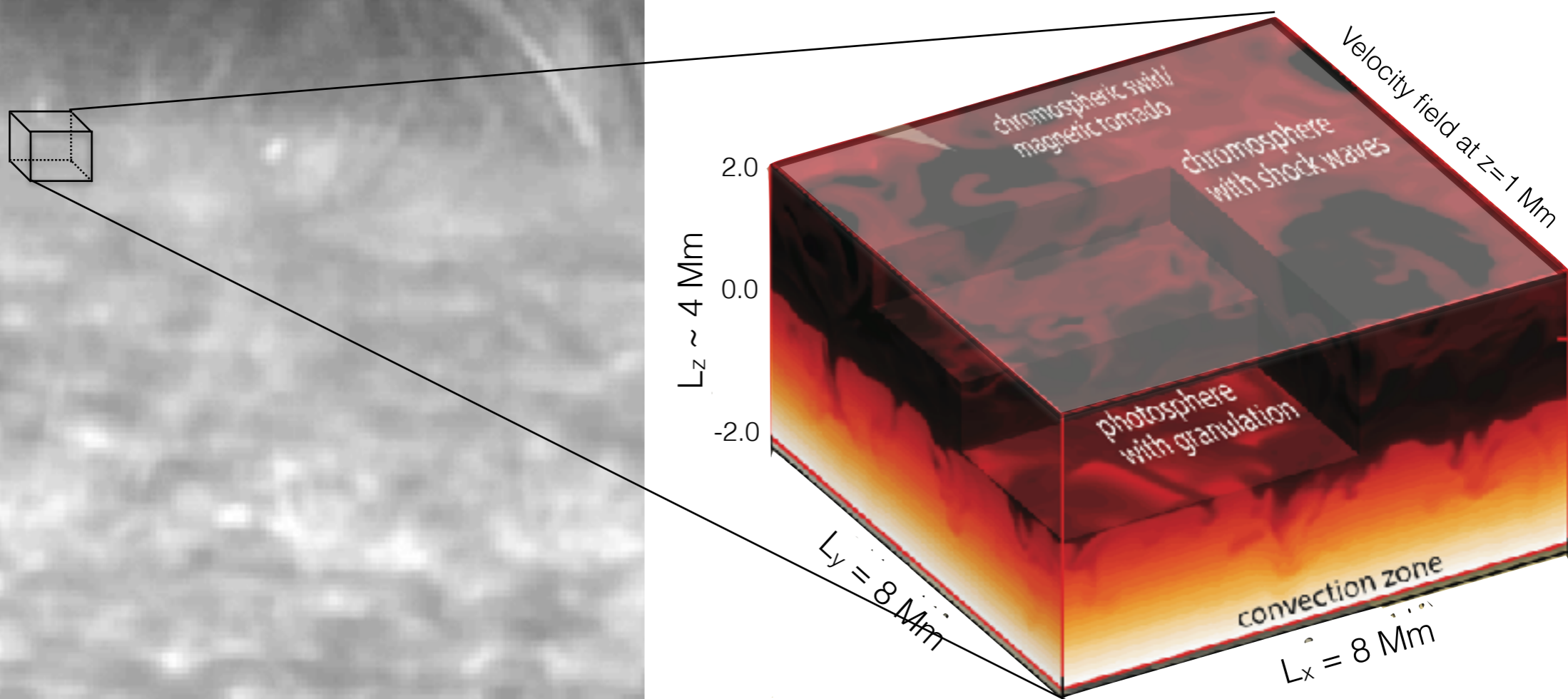
- a radial, non-circular flow

$$\mu \neq 0, \nu = 0 \longrightarrow P = -\frac{x+y}{r^2} \mu, Q = \frac{xy}{r^4} \mu^2$$

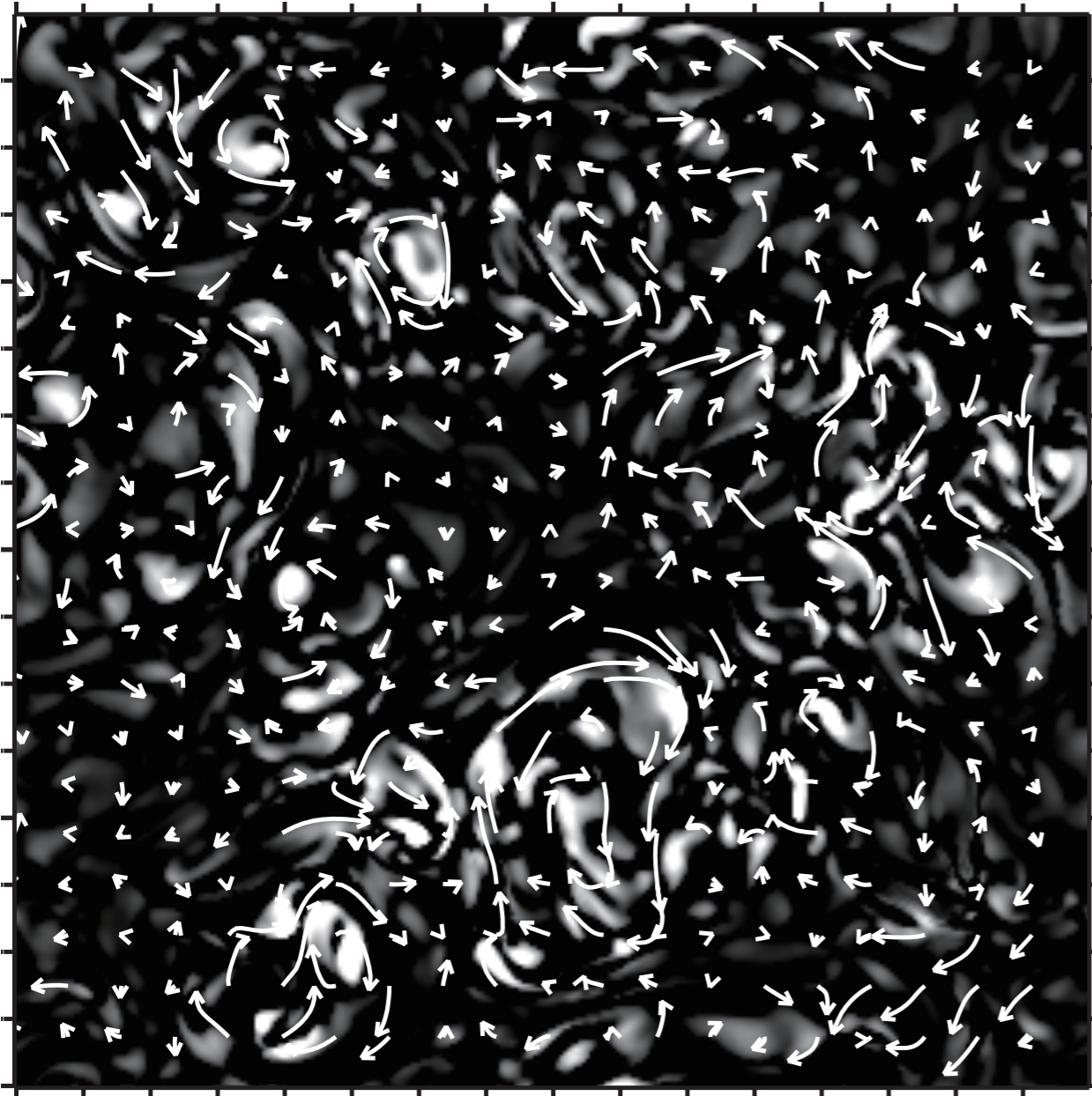
two distinctive real roots of $\lambda = \mu/r^2 x$ and $\mu/r^2 y$

Testing vortex detection algorithm by using solar atmospheric models

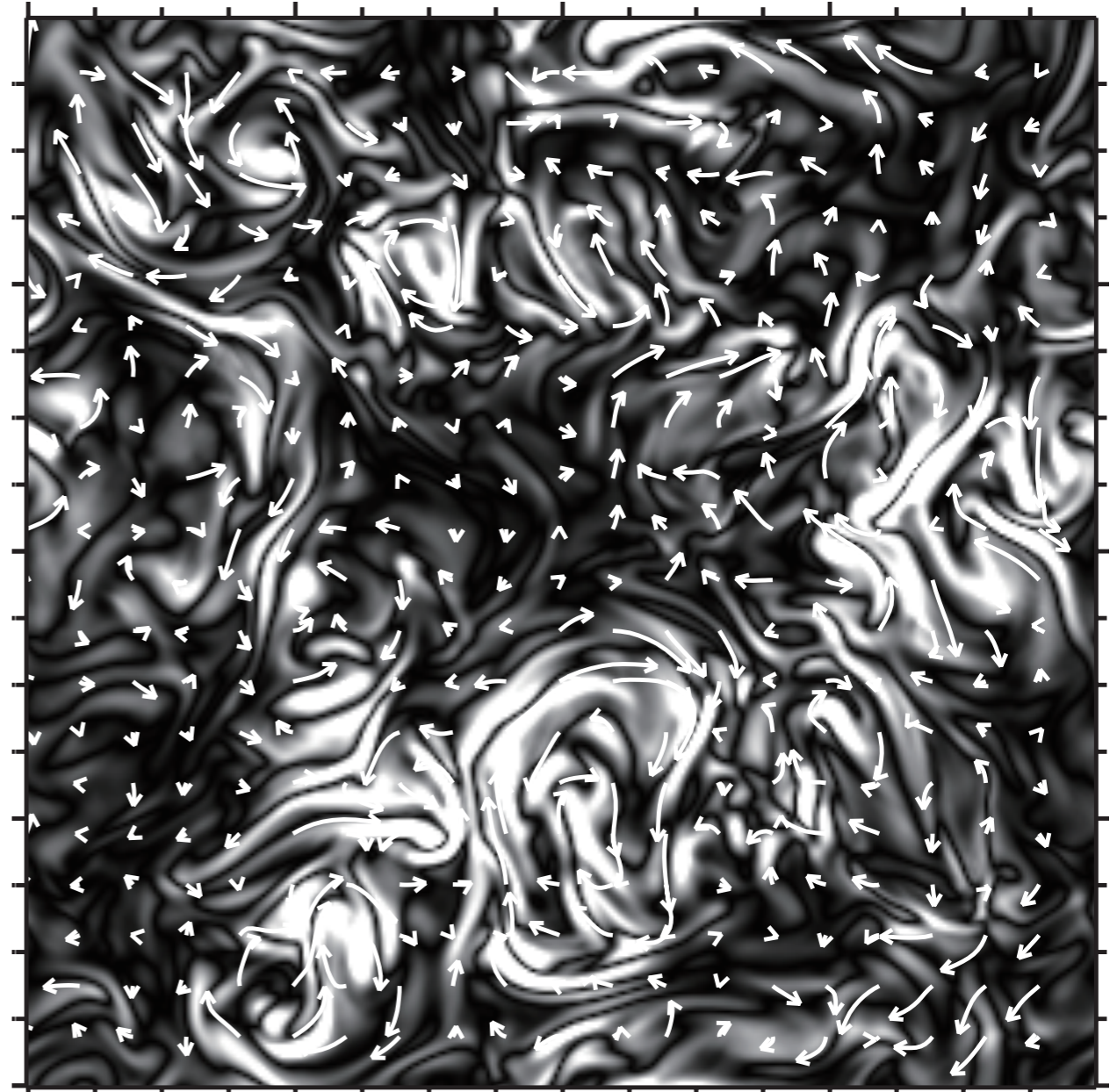
The velocity field at $z=1$ Mm is used as an input for testing the detection algorithm



Snapshots of vortical structure at the chromospheric height in the solar model atmosphere



Swirling strength

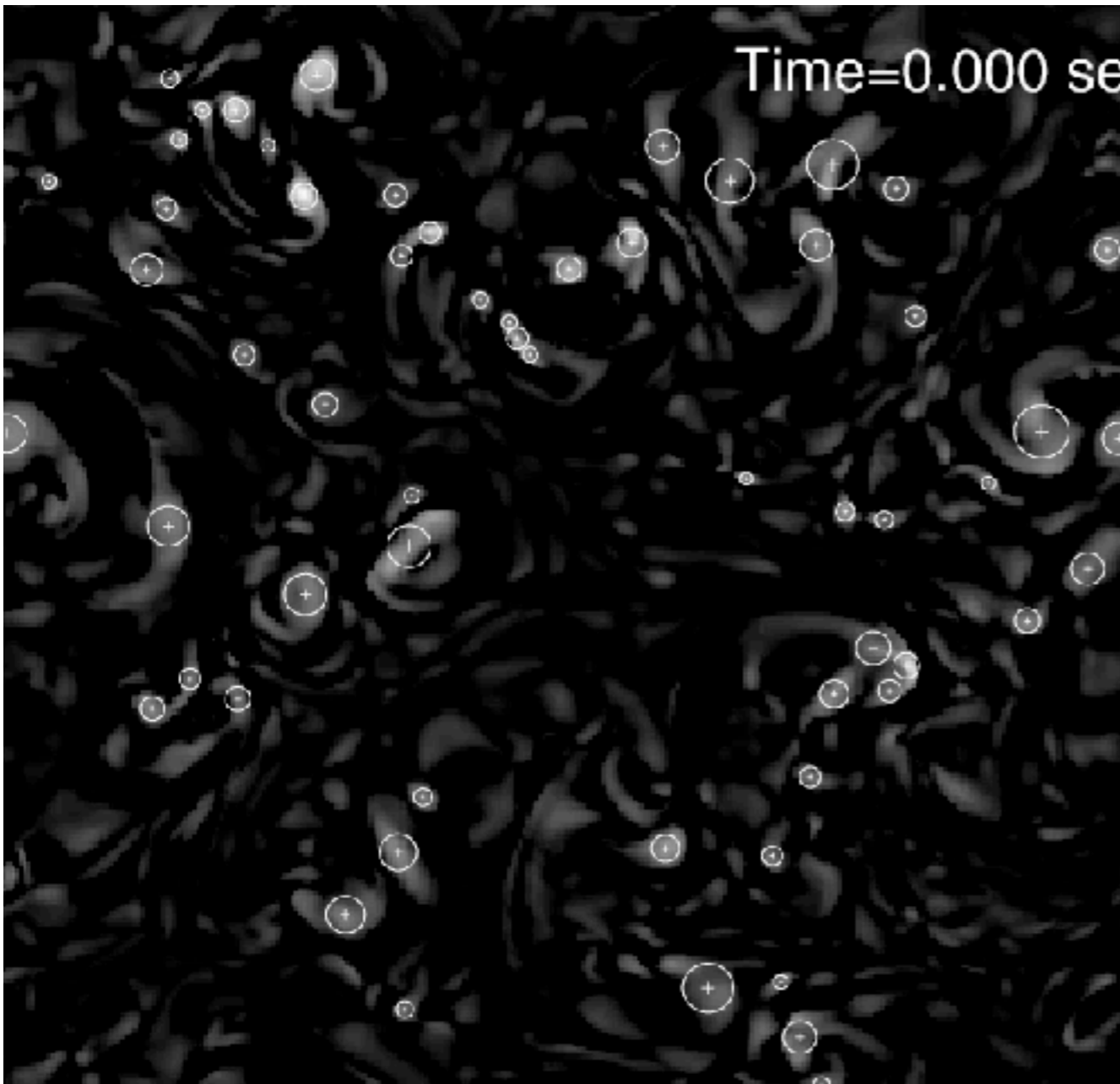


Vorticity

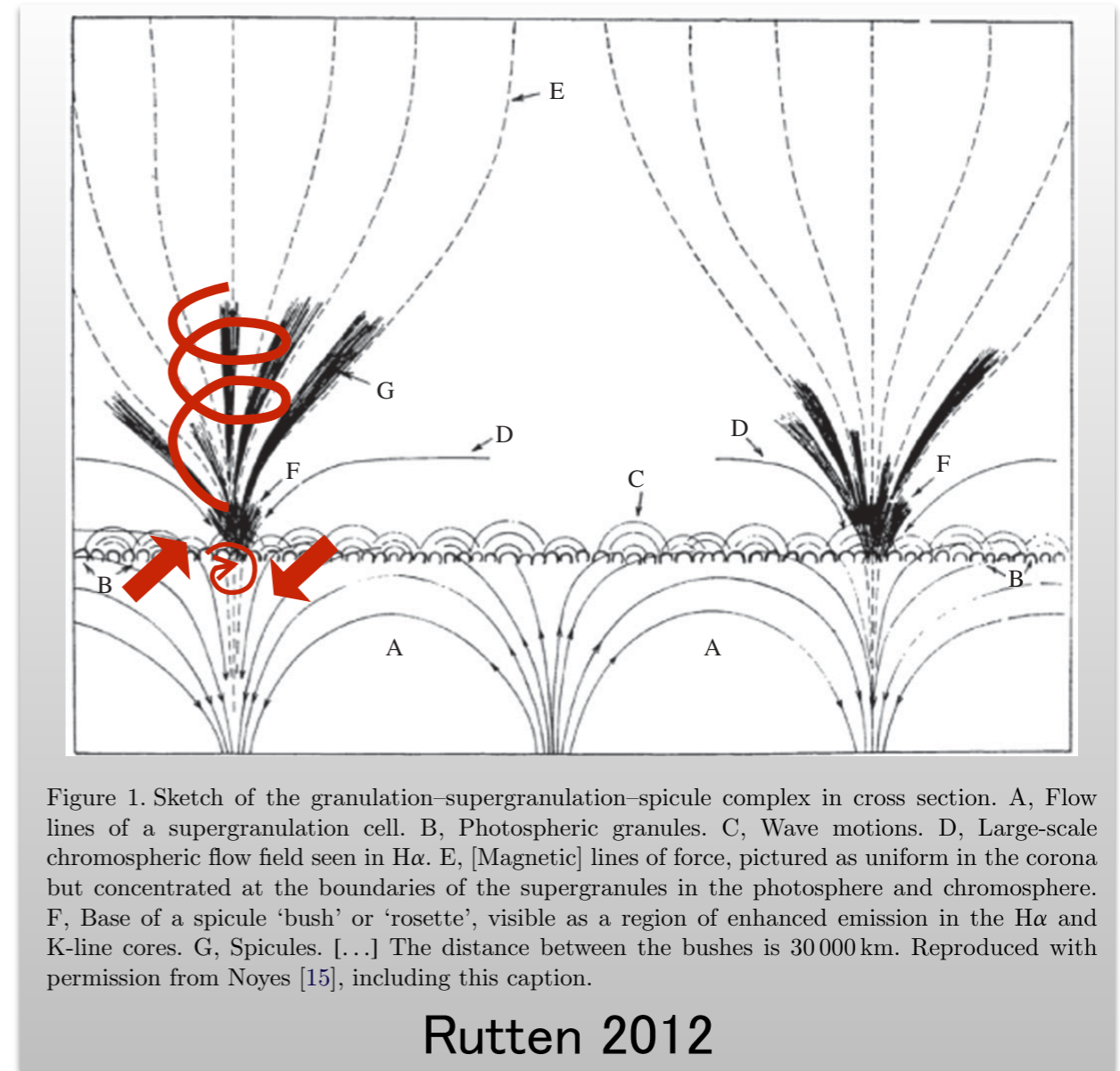
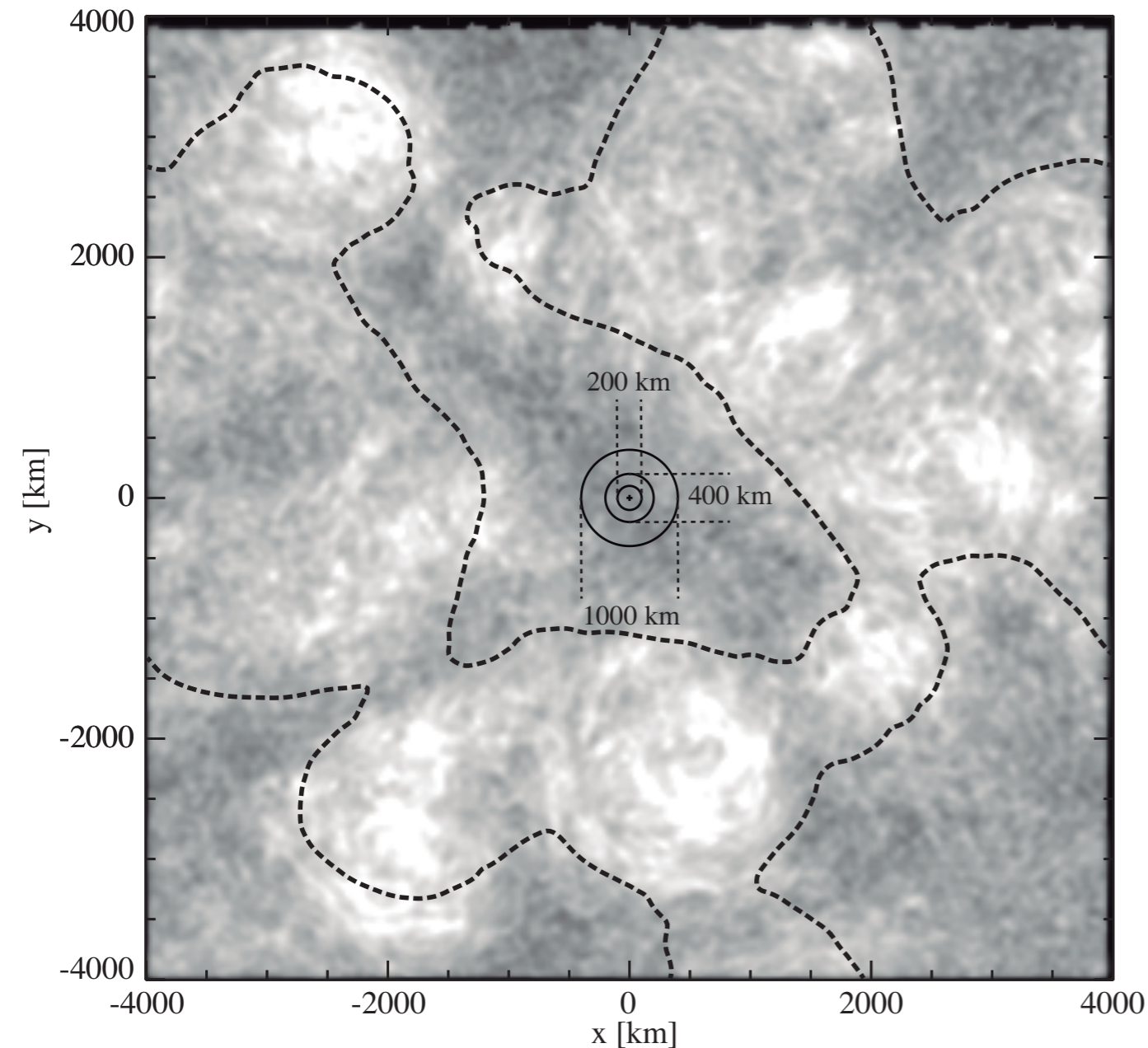
Comparison between swirling strength and vorticity

swirling strength

vorticity

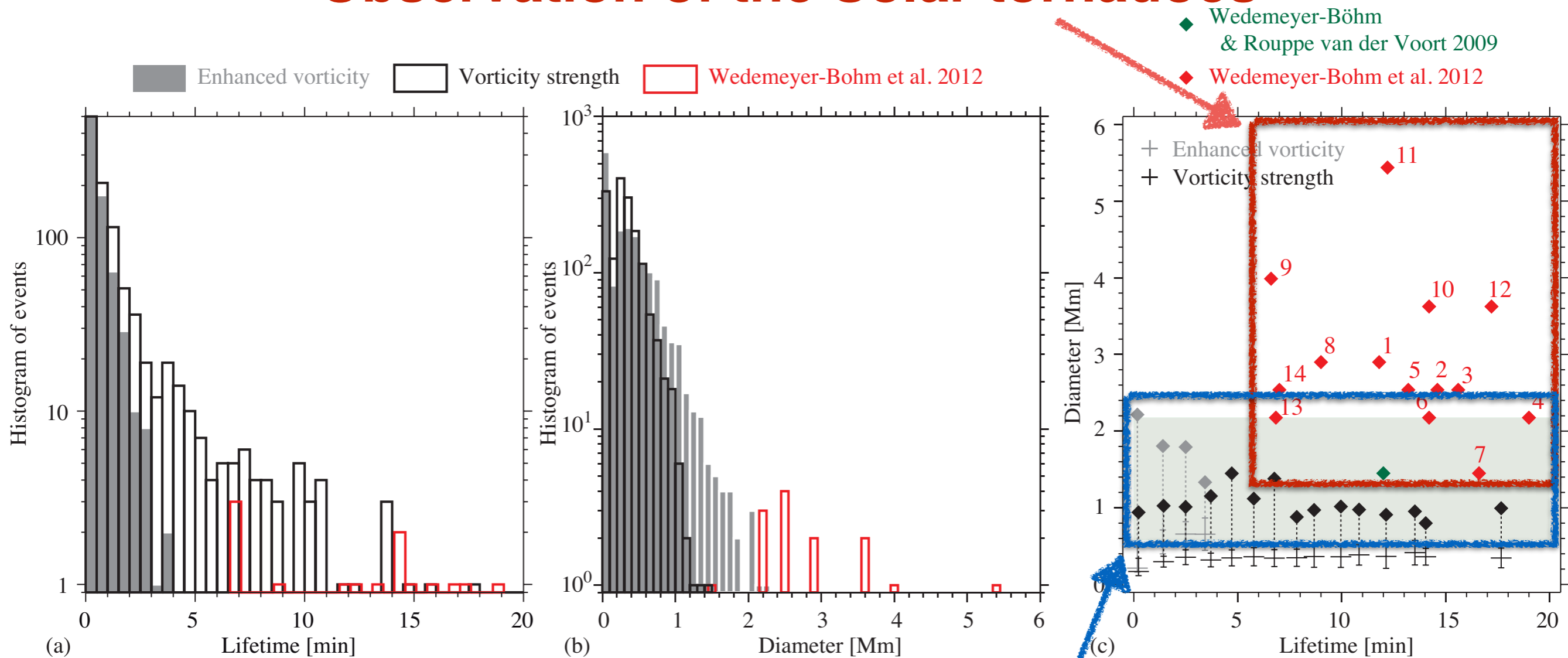


Correlation between vortical structure and enhanced magnetic structure



Comparison with the Solar observations

Observation of the Solar tornadoes

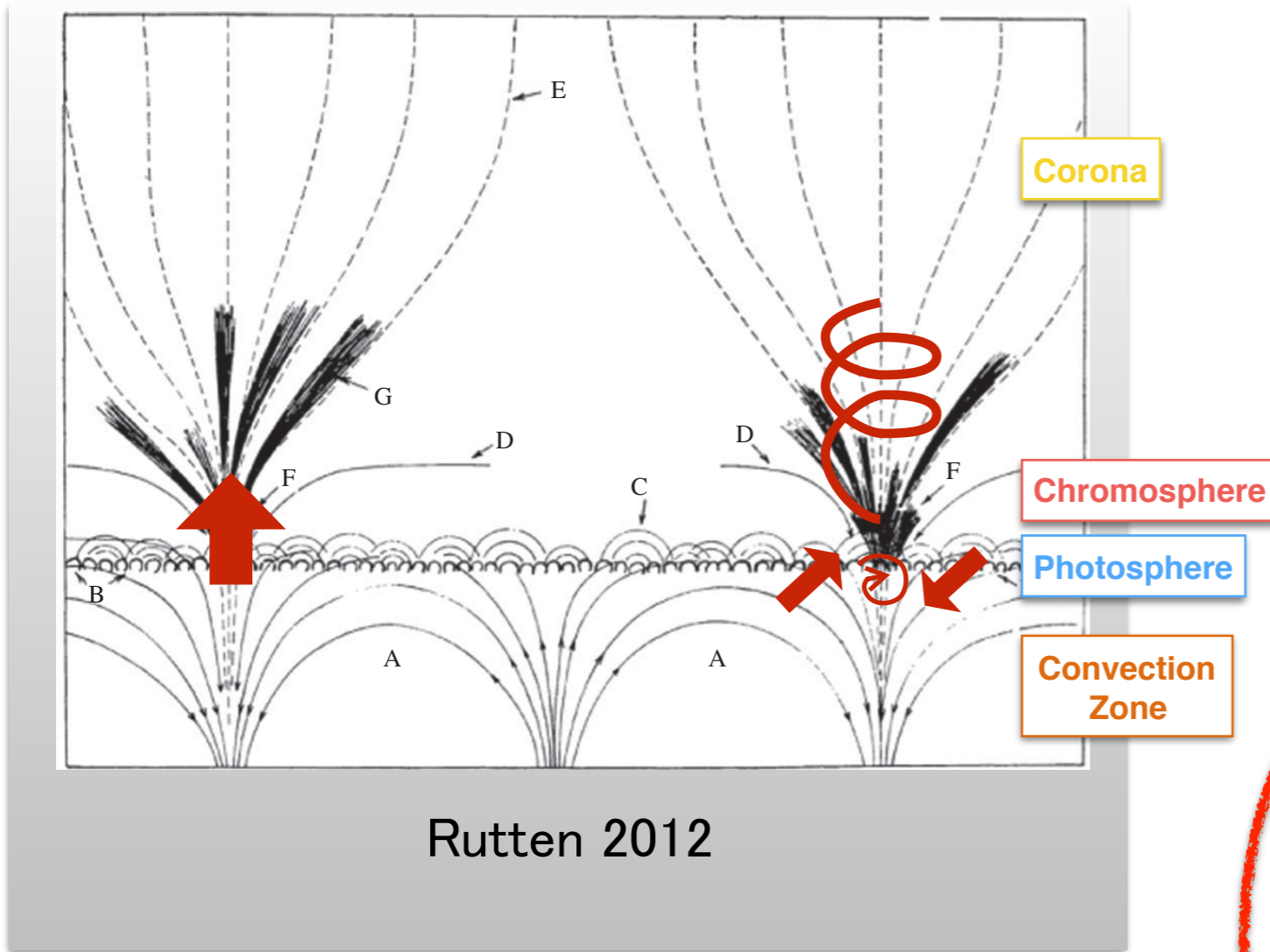


Our models

Reference

- Kato, Y., Wedemeyer, B., Vortex Flows in the Solar Chromosphere I. Automatic detection method, 2017, A&A

Summary



Magnetic flux sheath is a portal of energy transfer in the solar atmosphere

